

## Phase II-like murine trial identifies synergy between dexamethasone and dasatinib in T-cell acute lymphoblastic leukemia

Yuzhe Shi,<sup>1</sup> Melanie C. Beckett,<sup>1</sup> Helen J. Blair,<sup>1</sup> Ricky Tirtakusuma,<sup>1</sup>  
Sirintra Nakjang,<sup>1</sup> Amir Enshaei,<sup>1</sup> Christina Halsey,<sup>2</sup> Josef Vormoor,<sup>3</sup>  
Olaf Heidenreich,<sup>1,3</sup> Anja Krippner-Heidenreich<sup>3#</sup> and Frederik W. van Delft<sup>1#</sup>

<sup>1</sup>Wolfson Childhood Cancer Research Centre, Northern Institute for Cancer Research, Newcastle University, Newcastle upon Tyne, UK;  
<sup>2</sup>Wolfson Wohl Cancer Research Centre, Institute of Cancer Sciences, College of Medical, Veterinary and Life Sciences, University of Glasgow, Glasgow, UK and <sup>3</sup>Prinses Máxima Centrum voor Kinderoncologie, Utrecht, the Netherlands

*#AKH and FWvD contributed equally as co-senior authors.*

©2021 Ferrata Storti Foundation. This is an open-access paper. doi:10.3324/haematol.2019.241026

Received: October 21, 2019.

Accepted: March 4, 2020.

Pre-published: March 5, 2020.

Correspondence: *FREDERIK W. VAN DELFT* - frederik.van-delft@newcastle.ac.uk

---

## **T-ALL cell lines and Tissue Culture**

The cell lines used were available in-house, or kindly gifted by Dr M Mansour, UCL Cancer Institute, London, UK (ALL-SIL, CUTLL1, KOPTK1, MOLT16, DU.528, Loucy). All cell lines were authenticated before use. SUPT1, CUTLL1, MOLT4, Jurkat, HPB-ALL and CCRF-CEM were cultured in RPMI1640 with 10% fetal bovine serum (FBS; Thermofisher). HSB2, KOPTK1, ALLSIL, DU528 and MOLT16 were cultured in RPMI1640 with 20% FBS. 293T was cultured in DMEM with 10% FBS, 2 mM L-Glutamine and 1 mM Sodium Pyruvate (Sigma#S8636, Dorset, UK). The murine OP9-DL1 cell line was kindly provided by JC Zuniga-Pflucker, Toronto, Canada, and cultured in MEM $\alpha$  (ThermoFisher) with 10% FBS. Cell culture media and additives were obtained from Sigma unless stated otherwise.

## **Xenotransplantation of patient samples**

Patient-derived xenografts (PDXs) were harvested from the NOD.Cg-PrkdcscidIl2rgtm1wjl/SzJ (NSG, Charles River labs and bred in-house) mice after the engraftment of patient samples. PDXs were co-cultured ex vivo with OP9-DL1 in StemSpan Serum-Free Expansion Medium II (STEMCELL, UK) supplemented with human IL-7 (10 ng/ml) and SCF (100 ng/ml) (both PeproTech, UK).

## **Lentivirus Production and Cell Transduction**

Lentivirus was generated in 293T cells, seeding  $1 \times 10^6$  cells per 10 cm plate (Corning, USA) by co-transfection with a second-generation lentiviral vector pMD2.G and pCMV  $\Delta$ R8.91. For co-transfection, 5  $\mu$ g pMD2.G, 15  $\mu$ g pCMV  $\Delta$ R8.91 and 20  $\mu$ g of lentiviral vector were mixed to a final volume of 500  $\mu$ l containing 0.25 M CaCl<sub>2</sub>. This solution was slowly mixed with 500  $\mu$ l 2xHeBS (0.28 M NaCl, 0.05 M HEPES, 1.5mM Na<sub>2</sub>HPO<sub>4</sub>, pH 7.0) drop by drop. After thorough mixing, the mixture was left for 30-40 mins at room temperature. The 1 ml transfection mix was gently dropped onto a 293T monolayer of 25-35% confluency. On the 3rd day, after aspirating the 293T medium, the cells were carefully washed once with PBS and fresh cell culture medium was added. After culturing the cells for 72 hours, the supernatant containing lentivirus was harvested and filtered through a 0.45  $\mu$ m Syringe Filter (StarLab, UK).

The filtered supernatant of 293T containing the lentivirus was either added directly to T-ALL cells or concentrated prior to improve transduction efficiency. Lentivirus was centrifuged by ultra-centrifuge centrifugation (Beckman Coulter Optima XE-100, IN, USA) at 26,500 x g for two hours and re-suspended in an appropriate volume of 100ul – 1 ml cell culture medium. Cells were seeded in 48-well plates at  $1 - 2 \times 10^6$  cells per well and transduced in presence of 0.1% polybrene (8  $\mu$ g/ml) by spinfection at 900 x g for 50 mins. After spinfection the cells were cultured and the next day the majority of the lentiviral and polybrene containing supernatant was removed from the cells, before addition of fresh media and transfer of cells to a 24-well plate. 5 - 6 days post transduction, the transduction efficiency was measured by flow cytometry.

## **Targeted shRNA Screen**

A library of short hairpin RNA (shRNA) targeting PTCRA, LCK, FYN, ZAP70, CD3E and LAT was generated using the pLKO5d.SFFV.eGFP backbone (kindly provided by Dirk Heckl and Jan-Henning Klusmann, MHH Hannover<sup>1</sup> (Supplementary Table S3). Positive and negative controls comprising 18 shRNAs were selected based on in-house shRNA screens in a variety of cancers. ShRNA oligonucleotides (Sigma-Aldrich, UK) were annealed by heating to 95°C for 5 min and slow cooling to room temperature. ShRNA oligonucleotides were ligated into the Bsm1 restriction enzyme site of pLKO5d.SFFV.eGFP vectors. Sequences were verified using Sanger sequencing (Source Bioscience, UK).

T-ALL cell lines and PDX cells were transduced to an  $MOI \leq 0.3$ . In PDX LK203 and L963, a transduction efficiency of 7% and 3% respectively was obtained. Samples were collected at baseline, day 16, 30 and 40 for the *in vitro* screen and at baseline and endpoint for the *in vivo* screen. Cells were intrafemorally injected into NSG mice and harvested once mice began to exhibit clinical signs. Genomic DNA (gDNA) was extracted using the DNeasy Blood & Tissue Kit (Qiagen, UK) and quantified by Nanodrop ND-1000 (Thermo Scientific, UK), after which 825 ng was amplified with barcoding primers (Supplementary Table S2) by 30 cycles of PCR using Phusion Hot Start II DNA Polymerase (ThermoFisher#F549L, Paisley, UK). The resulting amplicons were sequenced by next generation sequencing (NGS) (Illumina MiSeq) at Newcastle University Genome Core Facility and analyzed by the Bioinformatic Support Unit (Supplementary Table S1 and S2).

### **Next Generation Sequencing and analyses**

Raw sequencing reads were trimmed at both ends up to the locations of barcode sequence before aligning to the reference shRNA barcodes using Bowtie2<sup>2</sup> with a zero mismatch tolerance. An in-house script was used to extract read counts from aligned sequence files. Differential representation analyses of aligned read counts from different screen datasets were performed as described in Dai et al. using edgeR<sup>3,4</sup>. In brief, read counts were normalized to adjust for library size differences across samples. The likelihood ratio test method based on generalized linear models (GLM) framework in edgeR was used to test for differential representation of shRNA barcodes.

For screen data from cell lines, time-course differential representation analysis with replicates was performed in order to identify shRNAs with changes in their abundance over time (days 0, 16, 30 and 40). The analysis was performed for each cell line independently. Depletion of shRNAs over time was allocated a negative slope of the regression line, whereas enrichment of shRNAs was allocated a positive slope.

For the primograft LK203 *in vitro* screen dataset, we treated samples from different time points (day 16 and day 30 with/without mesenchymal stem cell MSC) as non-baseline samples and tested for differential representation between the baseline samples and non-baseline samples.

To control for unwanted variation (e.g. biological, technical) between samples derived from the *in vivo* screen dataset, the RUVg approach was employed to estimate factors of unwanted variation under the assumption that our negative controls (i.e. non targeted control (NTC) and shRNA targeting RUNX1/ETO) had constant representation across samples<sup>5</sup>.

To adjust for this unwanted bias, the estimated factors of unwanted variation as well as the covariate of interest were both included in the model for differential representation analysis which was performed on upper-quartile normalized counts using the GLM approach from edgeR as described above. In this dataset, we tested for differential representation between baseline samples and samples either from spleen or bone marrow separately.

### **Flow cytometry**

For PhosFlow,  $1 \times 10^6$  cells were washed with cold PBA (PBS, 1% BSA and 0.05%  $NaN_3$ ), fixed in Cytofix Fixation Buffer (BD Bioscience) for 15 mins at 37°C, washed and permeabilized in PermBuffer III (BD Biosciences) for 30 mins on ice. For control and specific staining, mouse serum (Sigma Aldrich#M5905), PE-IgG1 control (R&D#IC002P, clone 11711), Alexa Fluor 647-IgG control (Biolegend#400130, clone MOPC-21), Alexa Fluor 647-LCK (BioLegend#628303, clone LCK-01) and PE-Src (Y418) (BD Biosciences#560094, clone K98-37) were used.

Cell cycle analysis was performed using propidium iodide or Hoechst 33342 (both Sigma Aldrich). Apoptosis assay was performed using PE-Annexin V/7-AAD (BD Biosciences) as per manufacturer's instructions or APC-Annexin V (Biolegend)/LIVE-DEAD Fixable Aqua (ThermoFisher).

Peripheral leukemia engraftment was assessed by incubating mouse blood with APC-huCD45 (HI30), PE-huCD7 (M-T701) and BV421-mCD45 (30-F11) (all from BD Biosciences) for 20 mins in the dark. Red cells were lysed using freshly prepared lysis buffer (155 mM NH<sub>4</sub>Cl, 12 mM NaHCO<sub>3</sub>, 0.1 mM EDTA) for 10 mins. Cells were stained for cell viability with LIVE/DEAD Fixable Aqua prior to fixation in 2% paraformaldehyde.

For PDX proliferation assays, PDXs were incubated with 5 μM Cell Trace Violet (CTV) (ThermoFisher#C34571, Paisley UK) for 20 mins at 37°C. Cell loading was stopped using FBS (10% final), cells were washed in PBS and reseeded in SFEM II medium with OP9-DL1 cells. Two weeks later, cells were separated from feeder cells by repetitive transfer of leukemic cells. BD FACSCanto™ II was used to assess CTV distribution at the excitation/emission of 405/450. Flow cytometry was performed on BD Calibur or BD LSRFortessa™ X-20 Attune NxT (ThermoFisher) and raw data were analysed by Flowjo (v10, Oregon, USA).

### **Competitive Assay**

*In vitro* T-ALL cells ( $1 \times 10^6$ ) were transduced with shRNA viral supernatant (500 μl). Transduction efficiency as demonstrated by GFP expression was determined at day 6. Five million cells were equally mixed with parental cells to generate approximately 50% GFP expression. Cells were kept in fresh medium and the GFP expression was assessed every three days. A relative GFP expression of 1 denotes a mixture of 50% GFP+ cells with 50% parental cells (ratio 1:1). Graphs were generated by using GraphPad Prism (version 6, CA, USA).

For the *in vivo* competitive assay MOLT4 cells were transduced with either pLKO5RFP657-shNTC (kindly provided by O Heidenreich) or GFP-shLCK#3 (see section Targeted shRNA screen). The cells were then mixed to give a 1:1 ratio of RFP : GFP.  $1 \times 10^7$  cells were injected into 5 NSG mice. 26 days post injection mice showed signs of ill health and were humanely killed. Samples were collected from bone marrow, spleen and liver. Flow cytometry determined RFP and GFP ratio of leukemia cells after propagation *in vivo*.

### **SDS-PAGE and Western Blot**

Proteins of whole cell lysates in Laemmli buffer (32.9 mM Tris-HCl pH 6.8, 13.15% glycerol, 1.05% SDS, 0.005% bromophenol blue) were separated by SDS-PAGE and transferred onto Polyvinylidenedifluoride membranes (Merck Millipore). The following primary antibodies were used: LCK (#2984, clone D88), p-SRC (Tyr416) (#6943, clone D49G4), p-LCK (Tyr505) (#2751), p-PLCγ1 (Tyr783) (#2821), PLCγ1 (#5690, clone D9H10) (all purchased from Cell Signalling), GAPDH (Cat#5G4, clone 6C5, Hytest, Finland) and Clathrin. Secondary antibodies were from Dako (CA, USA): Goat Anti-Mouse IgG HRP (P0447), Goat Anti-Rabbit IgG (P0448). For developing Immobilon Western Chemiluminescent HRP Substrate (Millipore) and the ChemiDoc MP Imaging System with Image Lab Software (Bio-Rad) has been used.

### **RNA extraction and quantitative real-time PCR**

RNA was extracted from  $5 \times 10^6$  cells using the RNeasy Mini Kit (Qiagen, UK). Briefly, cells were collected at 500 x g for 3 mins and lysed in RLT buffer with 1% β-mercaptoethanol. The cell lysates were transferred to a QIAshredder column and centrifuged at 8,000 x g for 2mins. The flow-through was mixed with 70% Ethanol and moved to the RNeasy mini-spin column. After the centrifugation, the

flow-through was discarded, and the column was washed twice with RW1 and RPE buffer respectively. Finally, the column was dried off by centrifugation at maximum speed for 2 mins. The RNA was dissolved in RNase-free water and eluted from the column by centrifugation at 8,000 x g for 2 mins.

The cDNA was synthesized according to manufacturer's protocol by RevertAid H Minus First Strand cDNA Synthesis Kit (Thermo scientific#1631, Paisley, UK). The primers for qRT-PCR (Supplementary Table S3) were ordered from Sigma Aldrich (Dorset, UK). Samples were run on Applied Biosystems ViiA 7 (ThermoFisher, Paisley, UK). Relative mRNA expression was expressed as 2-DCt.

### **Bioinformatics analysis Drug matrix synergy**

The threshold analysis of log Dexamethasone was used to identify the optimum threshold for this drug. We have started from the minimum value (-3) and maximum value (7) and added or subtracted one unite at the time respectably. Similar method was used to access the optimum threshold of Dasatinib. This time for the minimum value (-13) and maximum value of (4). The proportion significance of cases within the threshold and synergy was calculated using fisher's exact test.

### **Xenotransplantation experiments**

Mice used in this project were bred and housed in the Newcastle University Comparative Biology Centre under specific pathogen-free conditions. A flow hood (FASTER S.r.l, Cornaredo (MI), Italy) was used for sterilized manipulations or experiments. All mouse work was approved and followed Home Office Project License PPL60/4552 and carried out by researchers with Home Office Personal License under the Animal (Scientific Procedures) Act 1986. All mice were humanely killed by a schedule 1 method when they exhibited endpoints as specified by the license. For example, when tumors reached 1.5 cm in diameter, if they lost > 10% weight compared to controls for 3 consecutive days or 20% at any time, or displayed signs of ill health.

### **Mouse Toxicity Studies**

A pilot toxicity study in a small number of NSG mice was carried to explore the maximal tolerant dosing of dasatinib in combination with 1 mg/kg dexamethasone. Six healthy mice (three males and three females) were dosed daily (Monday to Friday) with one dosing of combined 1 mg/kg dexamethasone and dasatinib by intraperitoneal (IP) injection. Mice were examined and weighed daily upon the drug administration. The starting dose of dasatinib was 5 mg/kg. Later the dose increased to 10 mg/kg, 20mg/kg and 35mg/kg for the highest dose. The initial drug was dissolved in DMSO stock and subsequently diluted down in water. On the 3rd week of combination of 1 mg/kg dexamethasone and 35 mg/kg dasatinib, all six mice lost 10-15% of weights indicating that they could not tolerate this dose any more. Dosing was stopped and the weights were monitoring continuously for 10 days. Mice gain weights gradually afterwards and were back to their original weights. The maximal tolerant dosing for NSG mice is 35 mg/kg dasatinib with 1 mg/kg dexamethasone for three weeks.

### **Harvesting of Leukemic Cells from Mice**

Spleen samples were homogenized through a cell strainer and bone marrow samples were harvested by flushing the lumens with PBS or crushing bones with a pestle and mortar with PBS.

### **Histological examination of murine heads**

Murine heads were stripped of soft tissues and decalcified in Hilleman and Lee EDTA solution (5.5% EDTA in 10% formalin) for 3 weeks, then trimmed and put in fresh EDTA for 4 days. Samples were processed on a Tissue-Tek VIP processor using a routine overnight 17.5 hour cycle. Following paraffin wax embedding, 2.5µm sections were cut onto Poly-L-silane coated slides. Sections were then stained

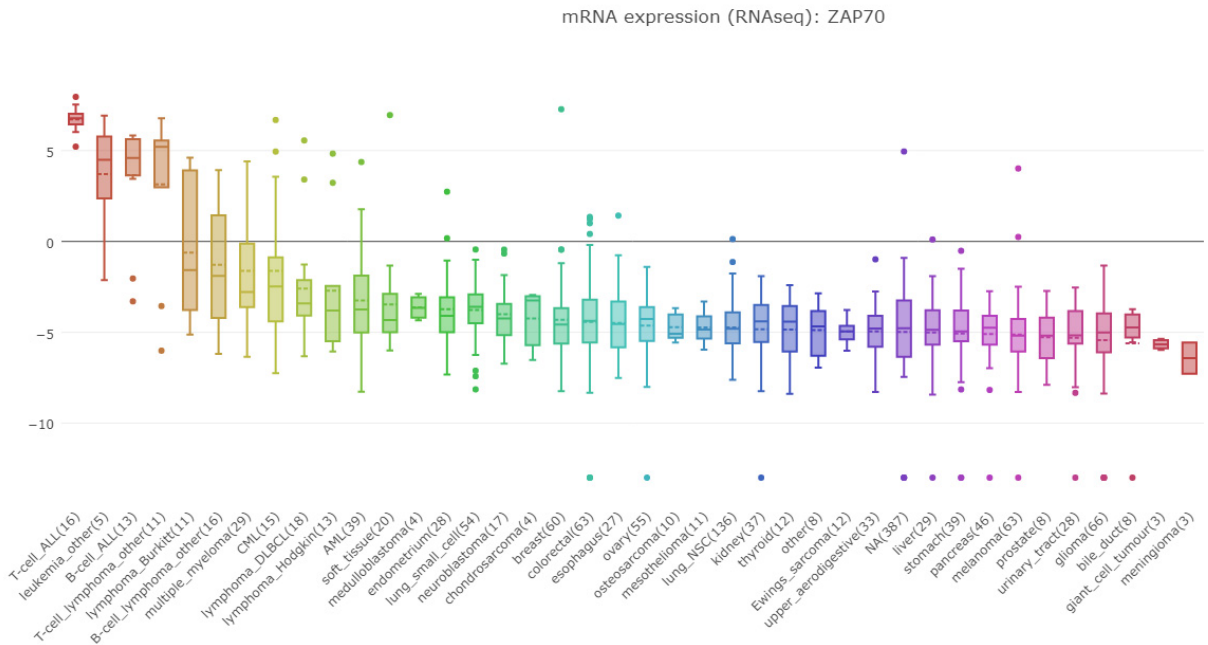
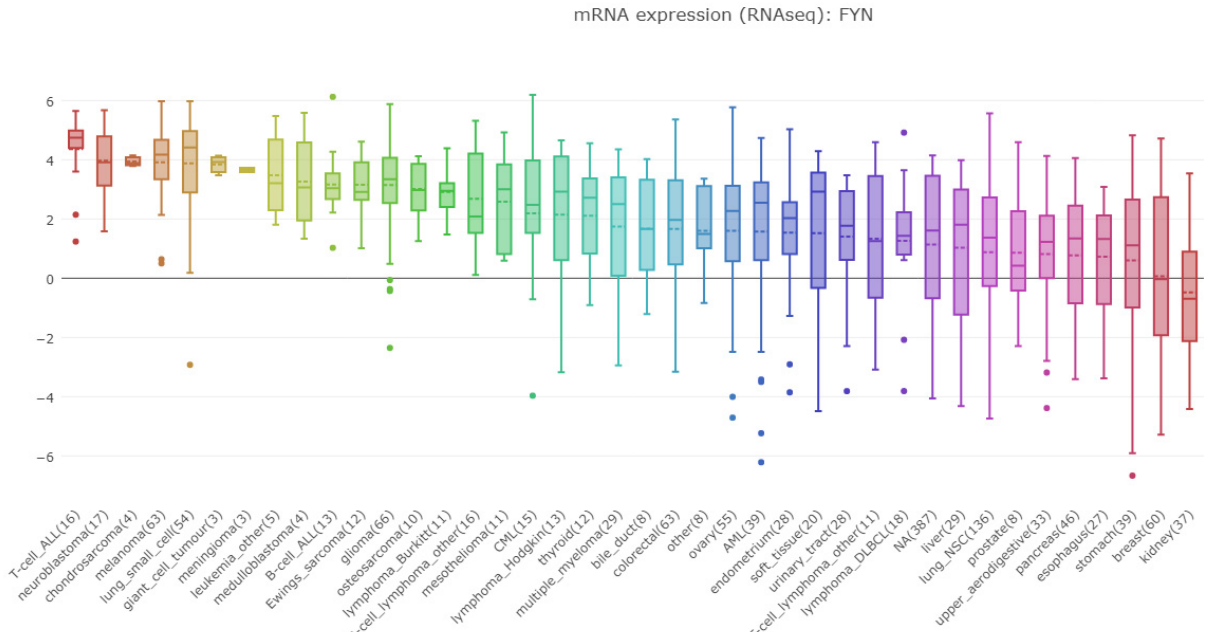
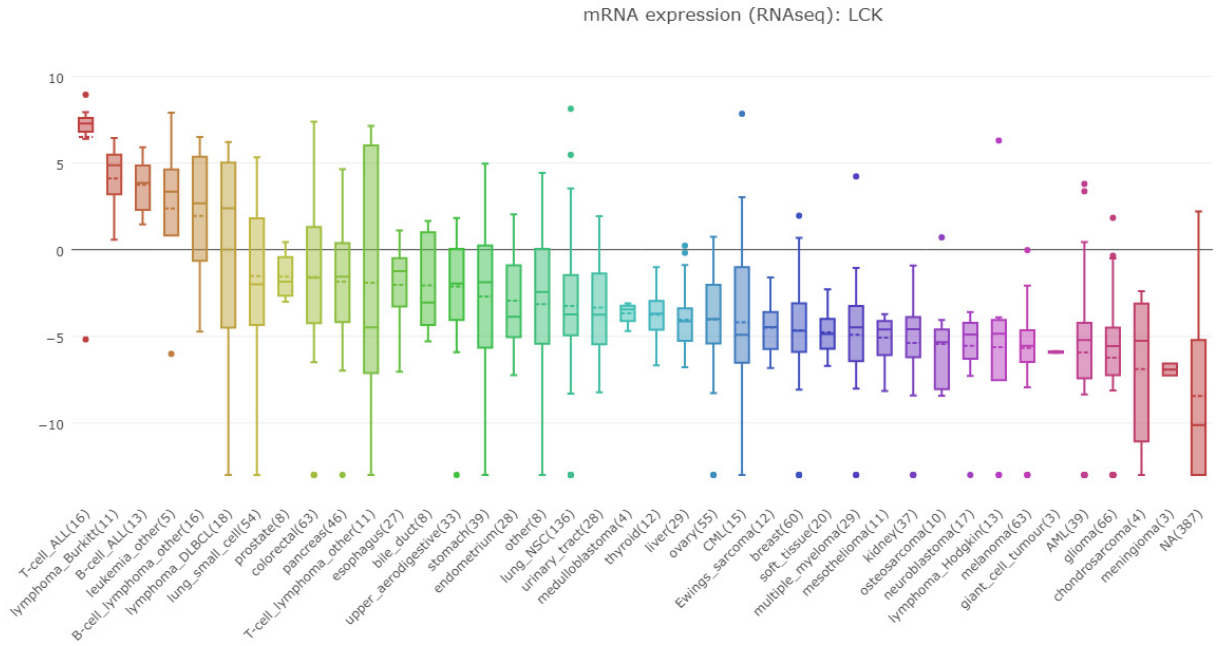
with Gill's haematoxylin and Putt's eosin (both made in house). Quantification of CNS infiltration was performed using a Hamamatsu Nanozoomer Digital Pathology slide scanner with digital slide management/image analysis software from Slidepath (Dublin). CNS infiltration was evaluated as previously described <sup>6</sup>, the maximal depth of CNS infiltrates was measured across 5 equally spaced brain sections per mouse and then averaged, all treatment allocations were blinded to the investigator performing the measurements.

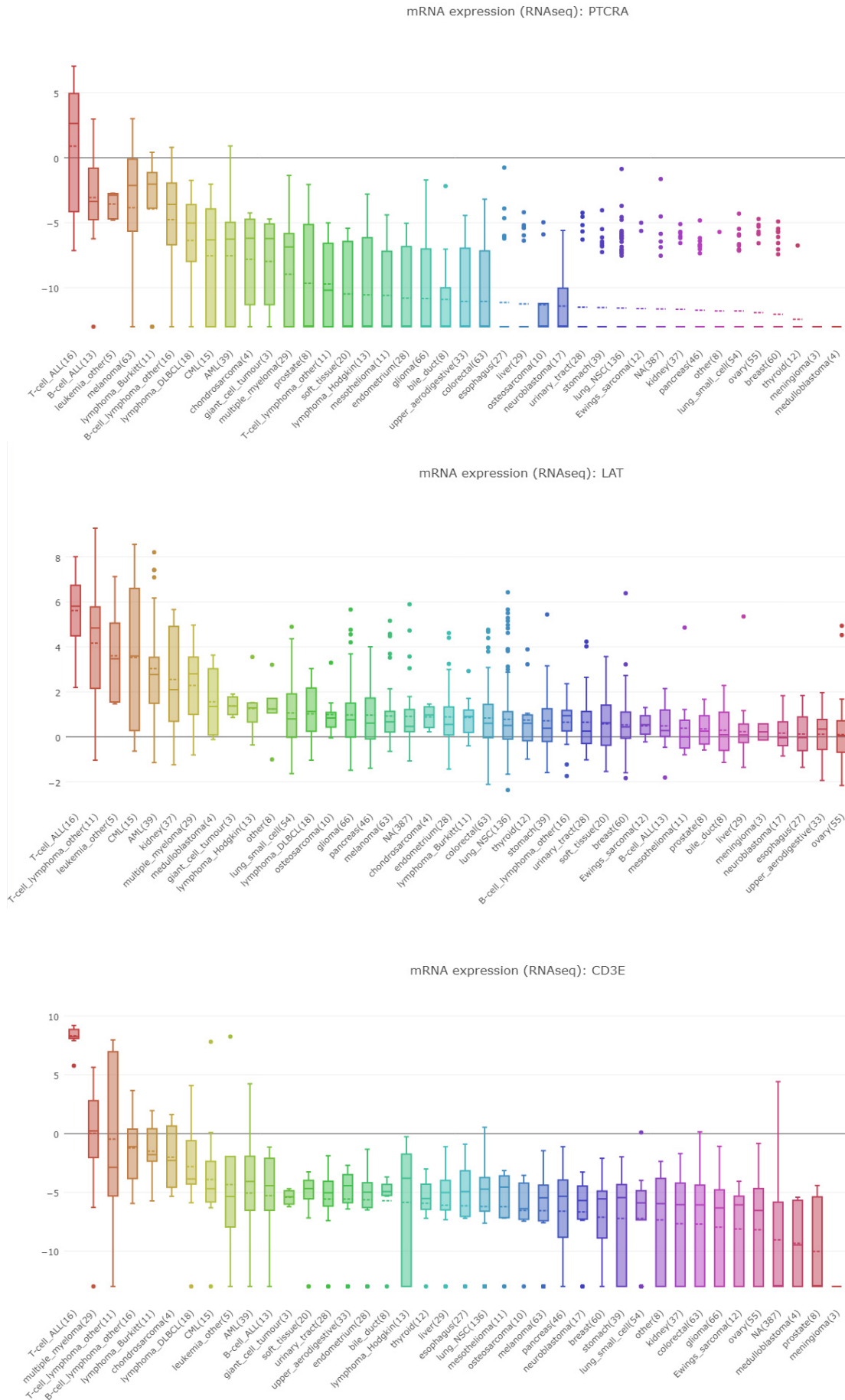
## References

1. Adams FF, Heckl D, Hoffmann T, et al. An optimized lentiviral vector system for conditional RNAi and efficient cloning of microRNA embedded short hairpin RNA libraries. *Biomaterials*. 2017;139:102-115.
2. Langmead B, Salzberg SL. Fast gapped-read alignment with Bowtie 2. *Nat Methods*. 2012;9(4):357-359.
3. Dai Z, Sheridan JM, Gearing LJ, et al. edgeR: a versatile tool for the analysis of shRNA-seq and CRISPR-Cas9 genetic screens. *F1000Res*. 2014;3:95.
4. Robinson MD, McCarthy DJ, Smyth GK. edgeR: a Bioconductor package for differential expression analysis of digital gene expression data. *Bioinformatics*. 2010;26(1):139-140.
5. Risso D, Ngai J, Speed TP, Dudoit S. Normalization of RNA-seq data using factor analysis of control genes or samples. *Nat Biotechnol*. 2014;32(9):896-902.
6. Irving J, Matheson E, Minto L, et al. Ras pathway mutations are prevalent in relapsed childhood acute lymphoblastic leukemia and confer sensitivity to MEK inhibition. *Blood*. 2014;124(23):3420-3430.

# Supplementary Figures

A

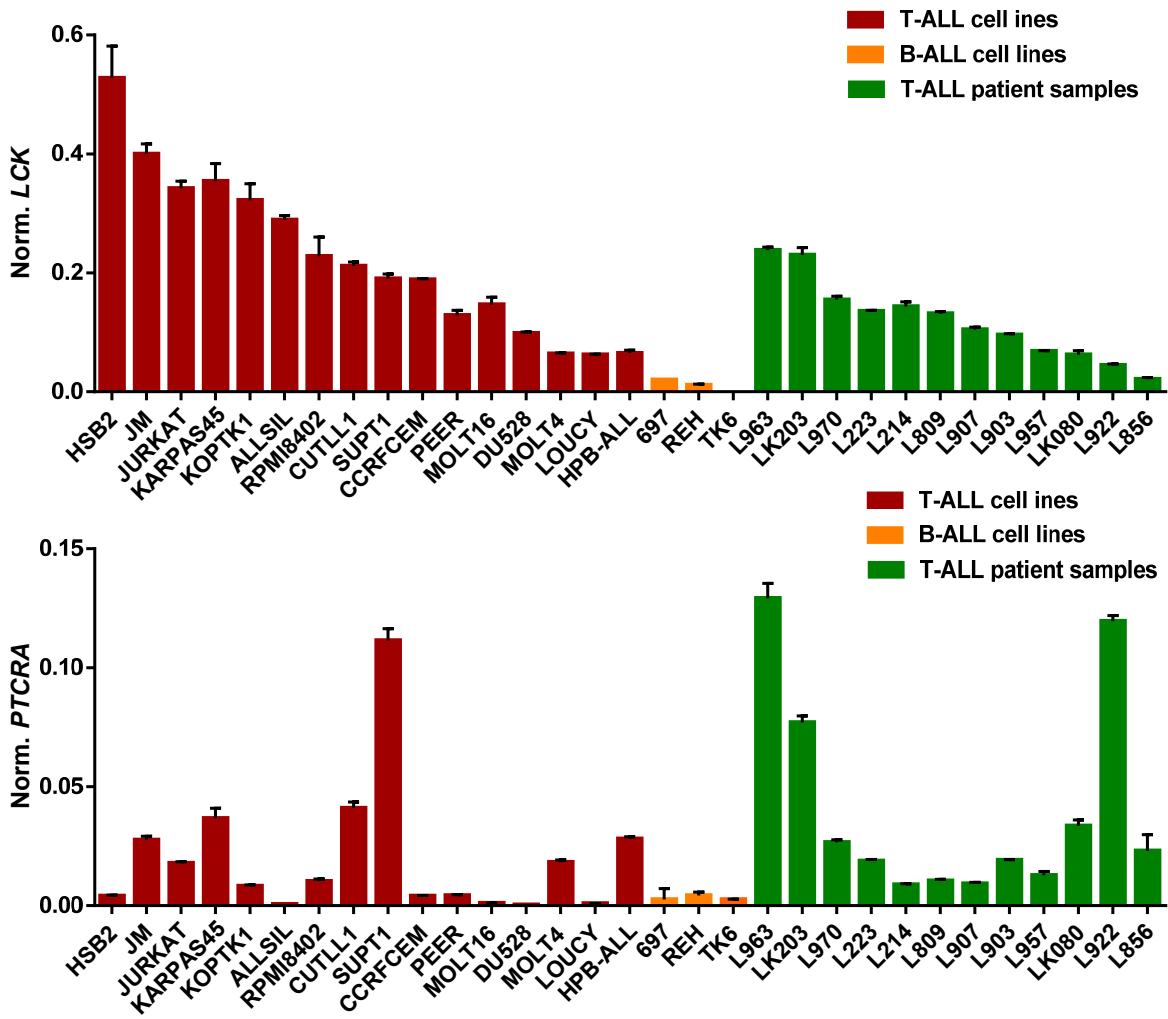




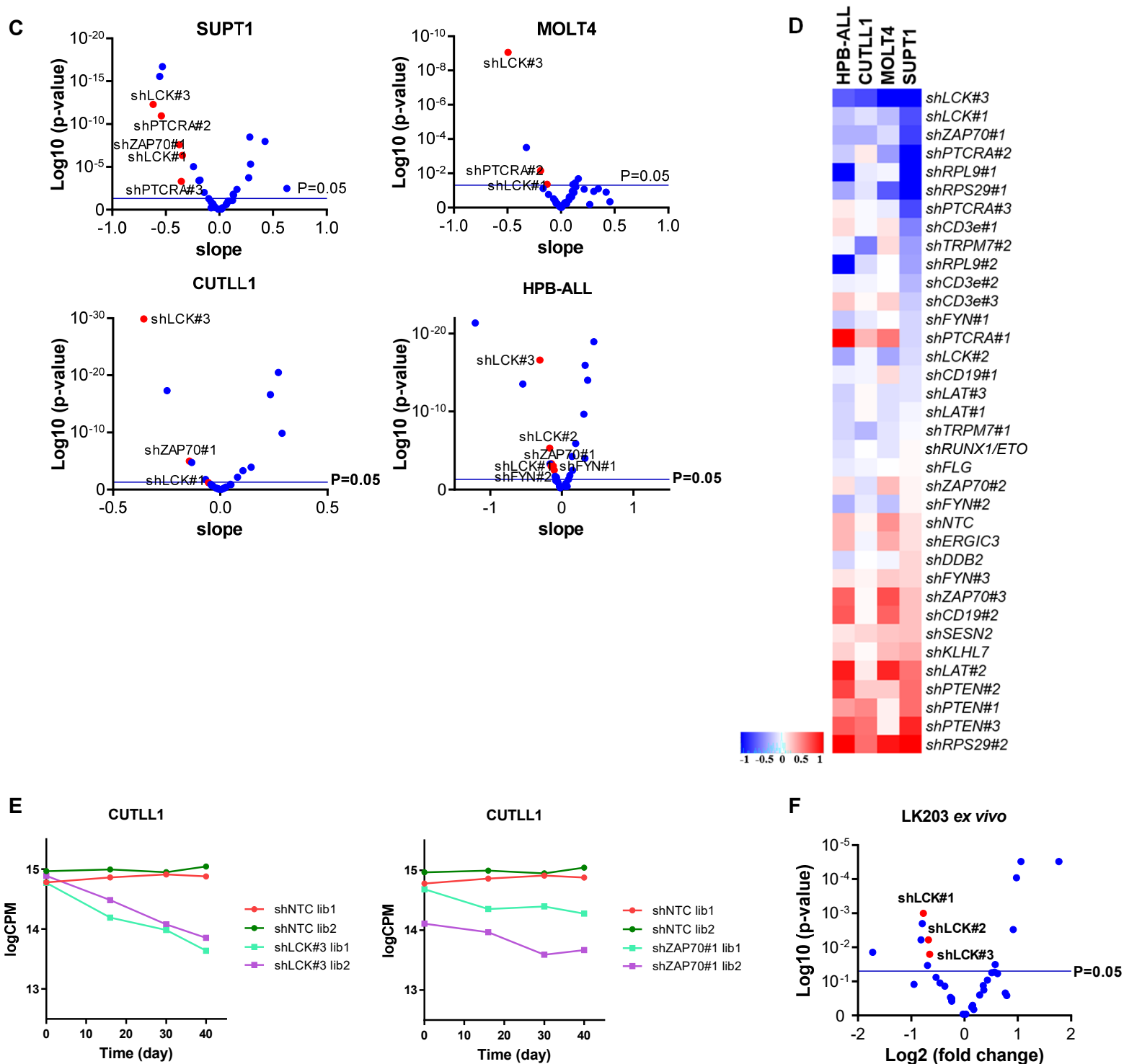
**Supplementary Figure 1A. Relative gene expression of targets in the shRNA screen.** *In silico* analysis, using the Cancer Cell Line Encyclopedia (CCLE), of gene expression of *LCK*, *FYN*, *ZAP70*, *PTCRA*, *LAT* and *CD3E* in a panel of cancer cell lines.



B

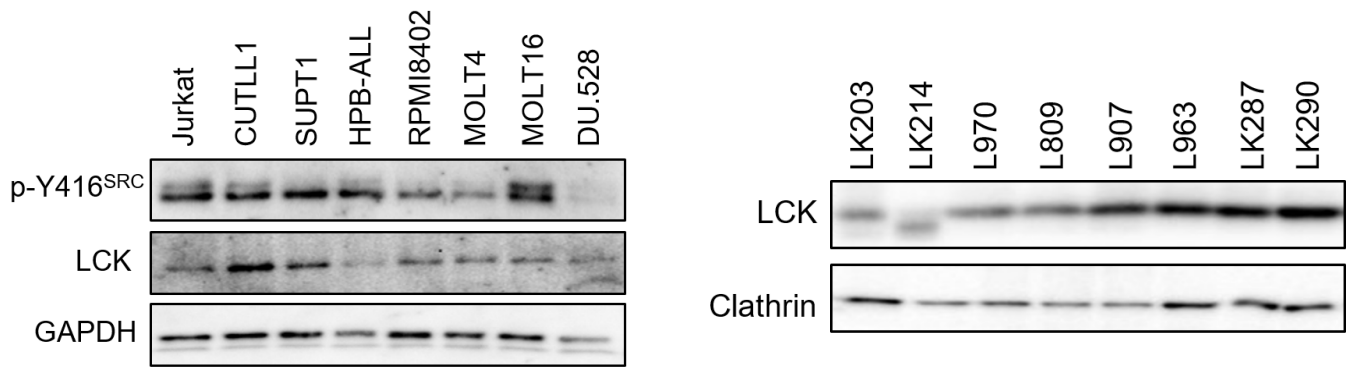


**Supplementary Figure 1B. Relative gene expression of *LCK* and *PTCRA* in a panel of cell lines and PDX samples.** *LCK* and *pTCRA* expression was determined in various T-ALL cell lines, 697 and REH (B-lineage ALL cell lines) and TK6 (lymphoblastoid cell line) by real time qPCR. *GAPDH* served as reference gene for normalization.

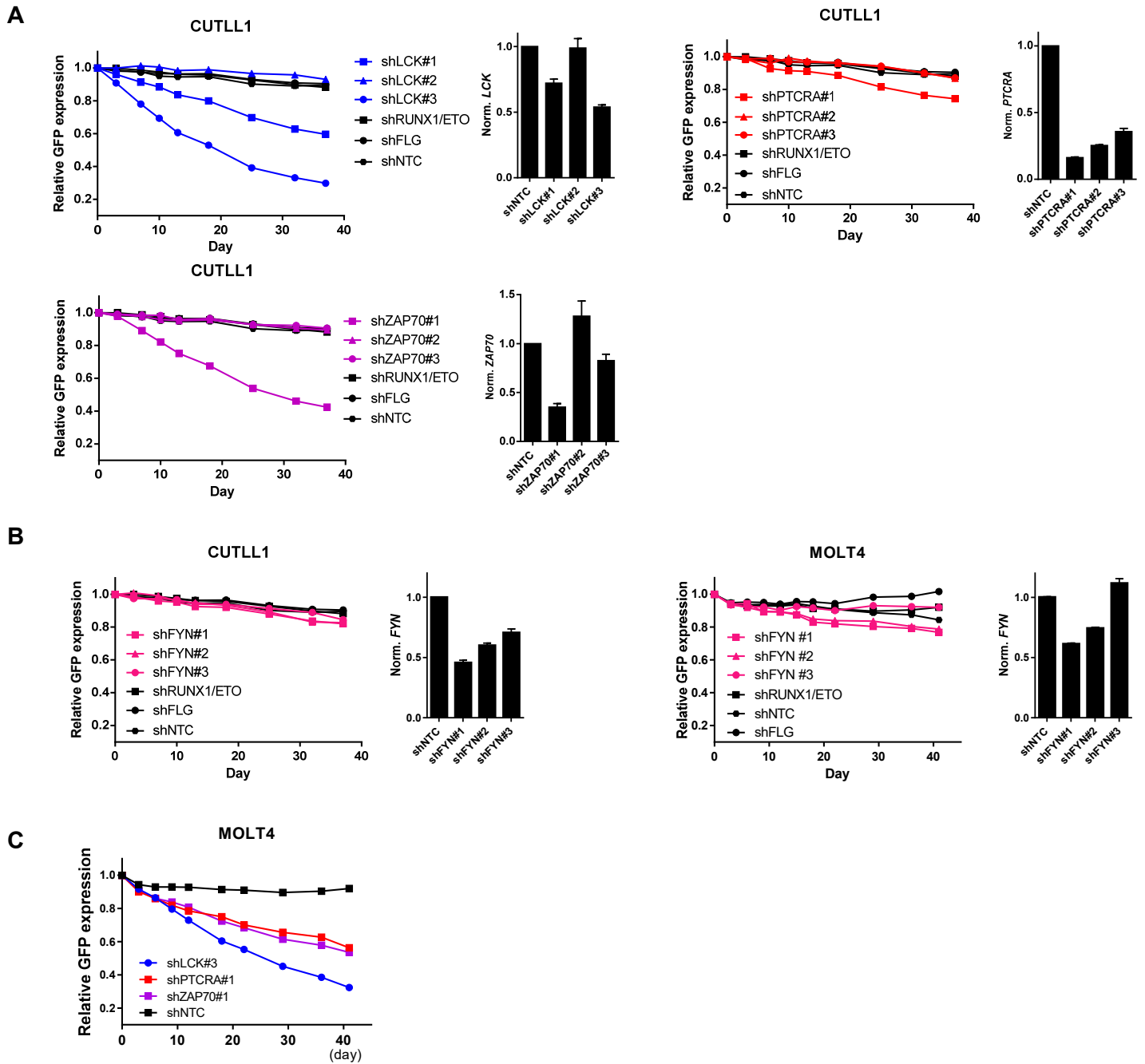


**Supplementary Figure 1C-F. Gradual depletion of shLCK#3 in T-ALL cell lines and PDX LK203 *ex vivo*.** Cells were lentivirally transduced with the pLKO5-shRNA library and the abundance of shRNAs were determined after 40 days (T-ALL cell lines) and 30 days (PDX LK203) growth *ex vivo*. (C) Volcano plots representing the change in shRNA representation over time (slope, x-axis) with negative values representing depletion. The y-axis represents the significance in enrichment or depletion of shRNA constructs (log<sub>10</sub> scale). Each dot represents an individual shRNA construct. Dots above the blue line have significantly changed ( $p < 0.05$ ). (D) Heatmap depicting relative representation of shRNA constructs after *in vitro* culture of 4 T-ALL cell lines (40 days). (E) Change in shRNA representation (logCPM) over time (days) for NTC (red, green), LCK and ZAP70 (lib 1 blue, lib 2 purple). shRNA derived from library 1 or 2. (F) Volcano plot representing the magnitude of the fold change (log<sub>2</sub>) in shRNA abundance derived from PDX LK203 leukemia cells on the x-axis. Each dot represents an individual shRNA construct. The y-axis represents the significance in enrichment or depletion of shRNA constructs (log<sub>10</sub> scale). Dots above the blue line are significantly depleted ( $p < 0.05$ ).

G



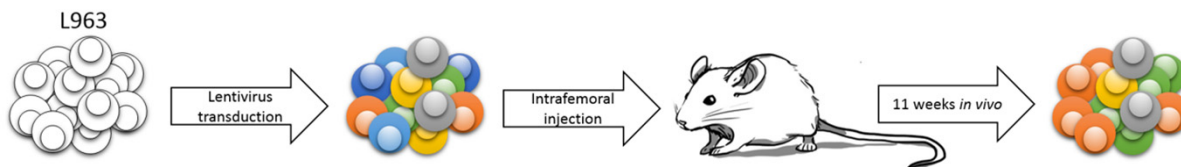
**Supplementary Figure 1G. LCK protein expression in T-ALL.** Western Blot analysis of LCK and p-Y416<sup>SRC</sup> protein expression in a panel of cell lines (left) and PDX samples (right). Comparative expression of housekeepers GAPDH and Clathrin is shown.



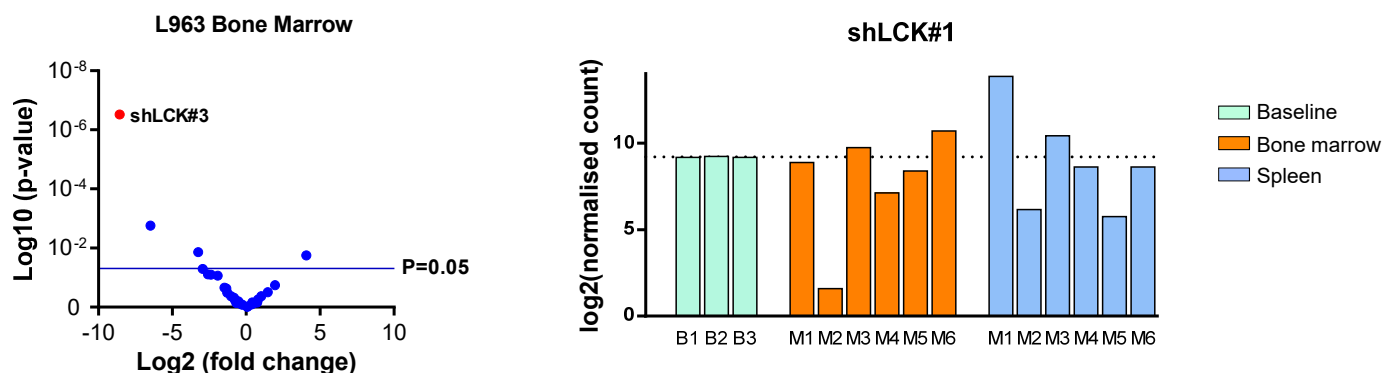
**Supplementary Figure 2. Competitive assays underline a critical role for LCK in T-ALL cell proliferation.**

(A) T-ALL cell line CUTLL1 was transduced with GFP expressing shLCK (blue), shZAP70 (purple), shPTCRA (red) or shNTC (black; RUNX1/ETO, FLG, NTC) expressing constructs. The cells were seeded in a 1:1 ratio with non-transduced parental cells *in vitro*. Cells were cultured and analyzed repetitively for the presence of GFP+ cells over a time period of 40 days. A relative GFP expression of 1 denotes a mixture of 50% GFP+ cells with 50% parental cells (ratio 1:1). A value of 0.5 means GFP+ cells represent 25% of total cells (ratio 1:4). Three separate shRNAs (#1,2,3) were used to target LCK, PTCRA and ZAP70. The knockdown efficiency at mRNA level is indicated in black bars on the right side of each proliferation plot. (B) CUTLL1 and MOLT4 cells were transduced with GFP expressing shFYN (pink) or shNTC (black) constructs and seeded in a 1:1 ratio with non-transduced parental cells *in vitro*. Cells were cultured and analyzed repetitively for the presence of GFP+ cells over a time period of 40 days. The knockdown efficiency at mRNA level is indicated in black bars on the right side of each proliferation plot. (C) MOLT4 cells were lentivirally transduced with shNTC (non-targeting control), shLCK#3 (blue), shPTCRA#1 (red), or shZAP70#1 (purple) expression constructs and seeded in a 1:1 ratio with non-transduced parental cells *in vitro*. Cells were cultured and analyzed repetitively by flow cytometry for the presence of GFP+ cells over a time period of 40 days.

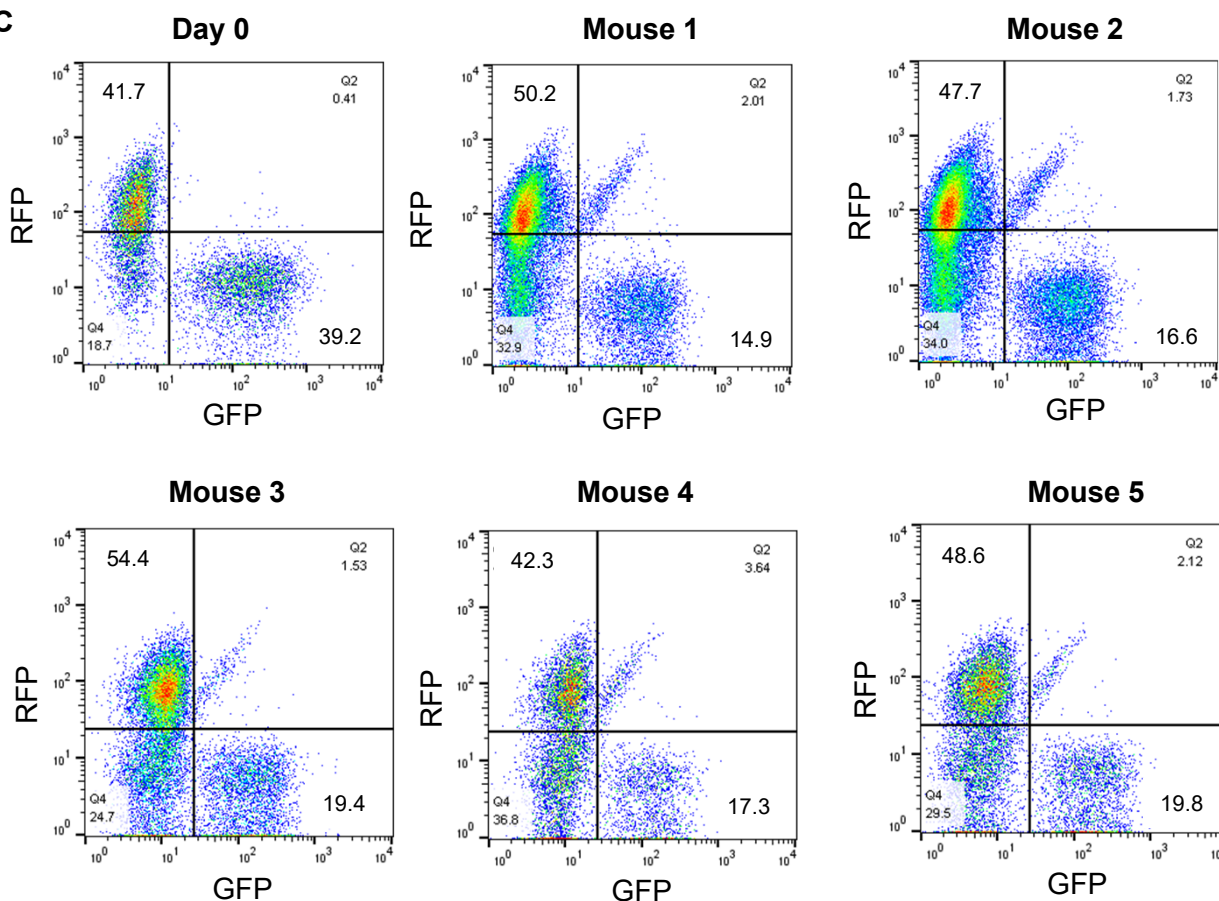
**A**



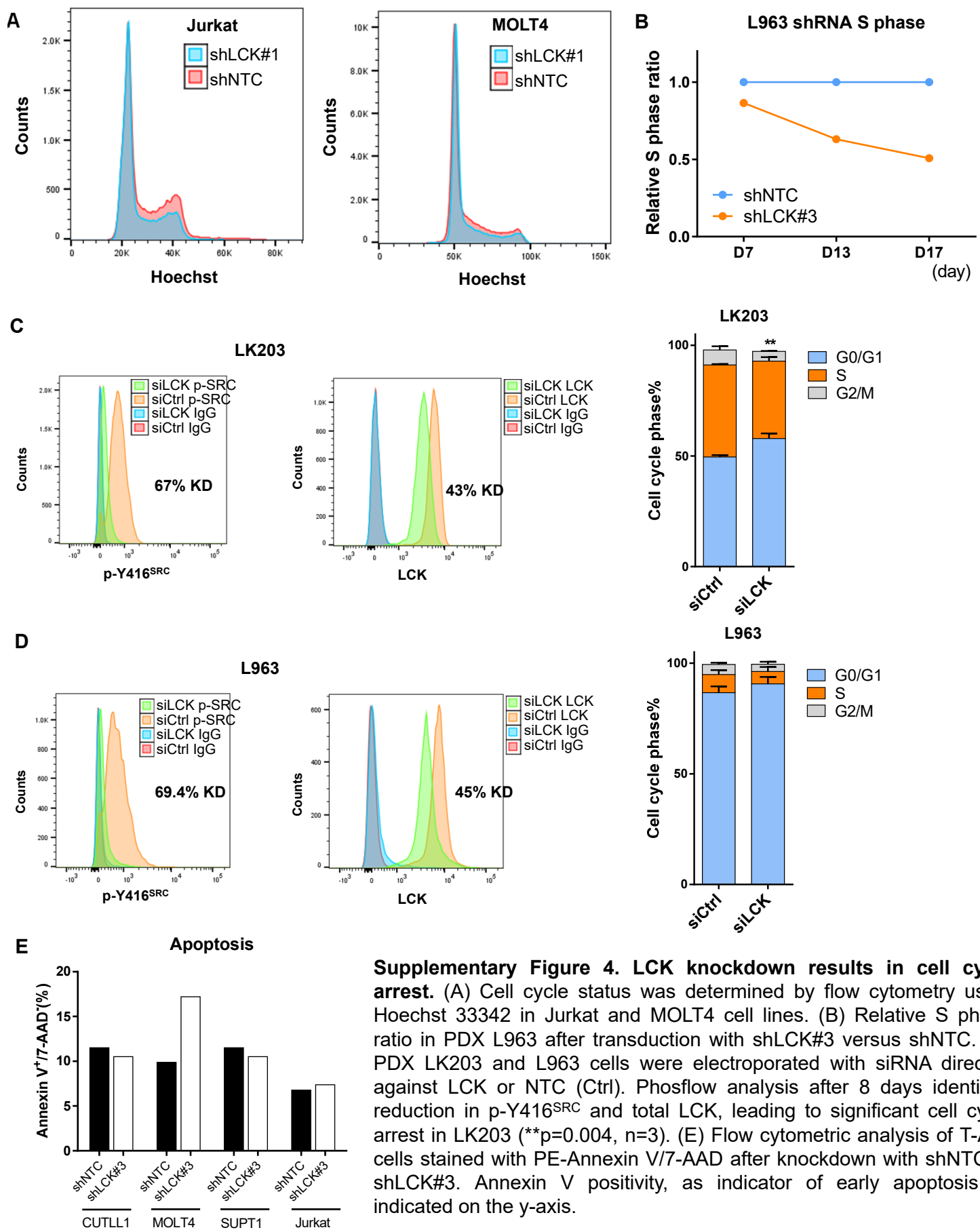
**B**



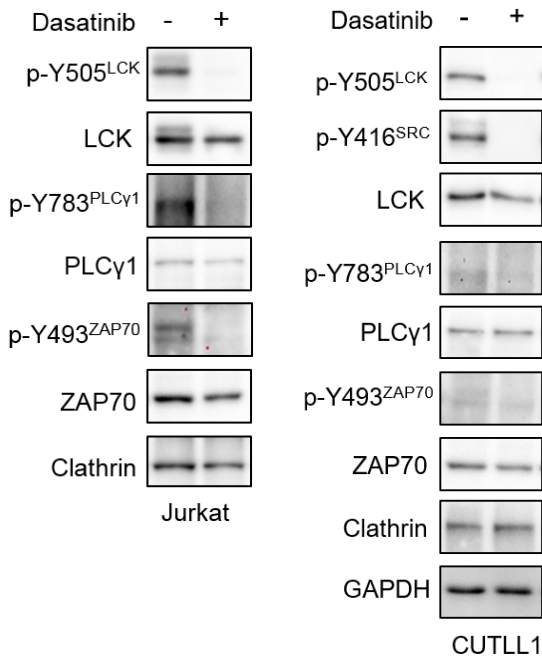
**C**



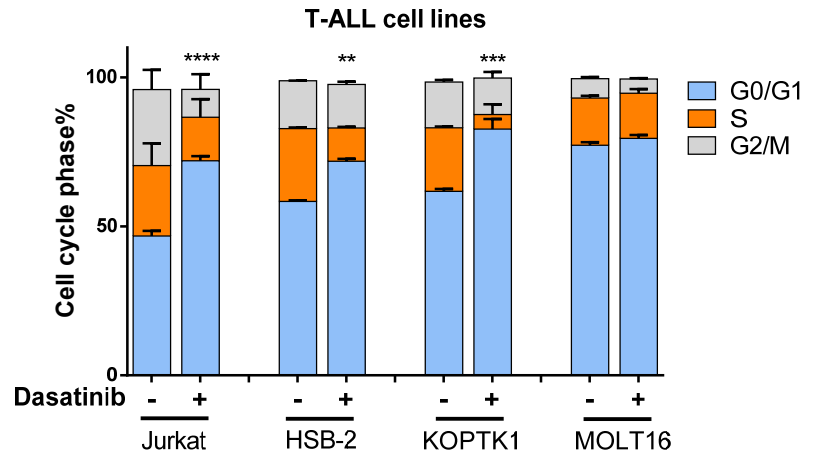
**Supplementary Figure 3. Targeted shRNA screen identifies critical role for LCK in T-ALL progression in immunocompromised NSG mice.** (A) Schematic representation of the *in vivo* targeted shRNA screen. (B) Volcano plot representing the magnitude of the fold change ( $\text{log}_2$ ) in shRNA abundance in PDX L963 bone marrow on the x-axis. shLCK#3 (red dot) represents the shRNA construct with most significant depletion in bone marrow. Bar plot of the normalized shLCK#1 sequencing reads ( $\text{log}_2$ ) in leukemic cells derived from the bone marrow (orange) or spleen (blue) of 6 individual mice (M1-6), relative to the frequency of these reads before transplantation (green, base line B1-3). (C) Flow cytometric analysis of representation of shNTC (red fluorescent protein, RFP) or shLCK#3 (GFP) constructs in MOLT4 *in vivo* competitive outgrowth assay. MOLT4 cells were derived from splenic tissue.



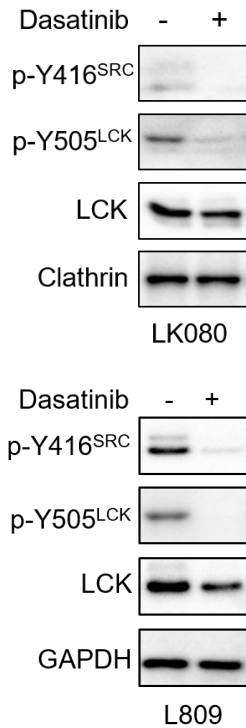
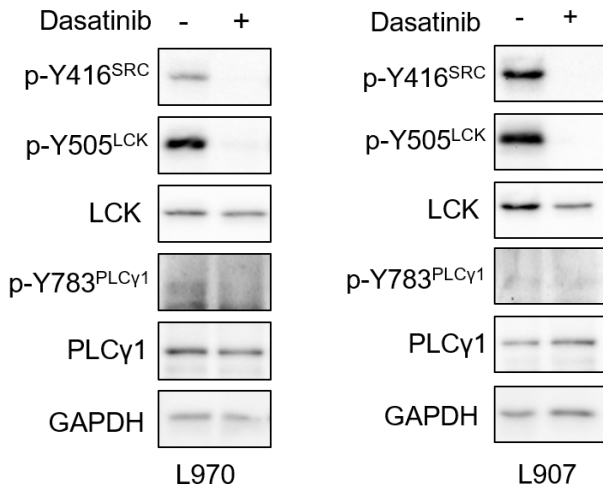
**A**



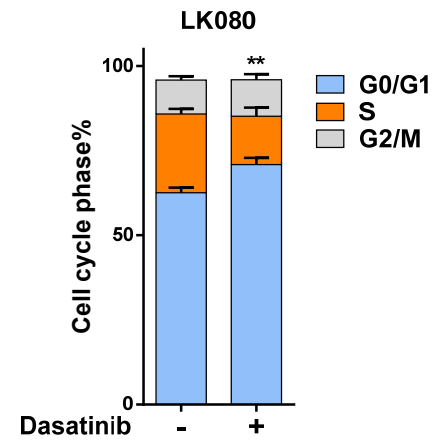
**B**



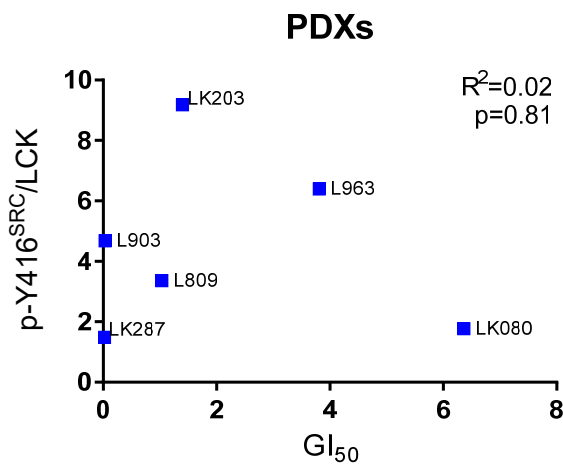
**C**



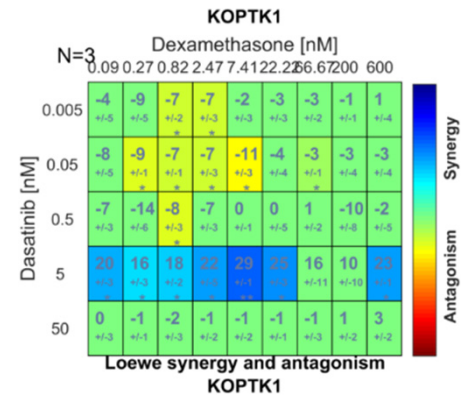
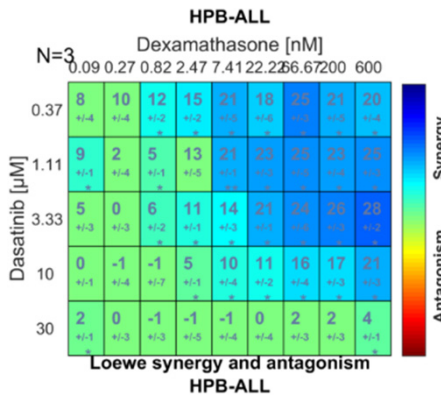
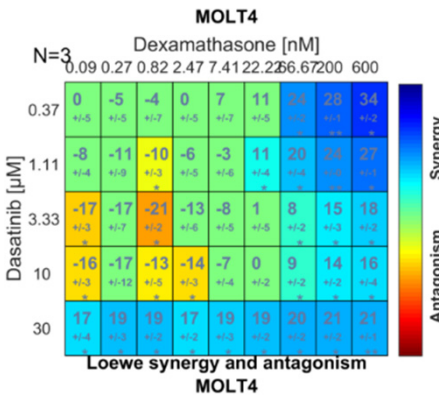
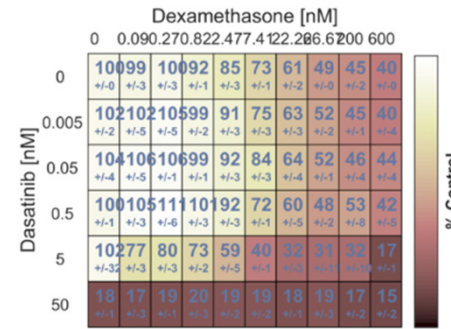
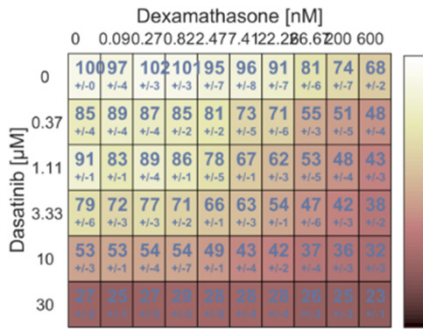
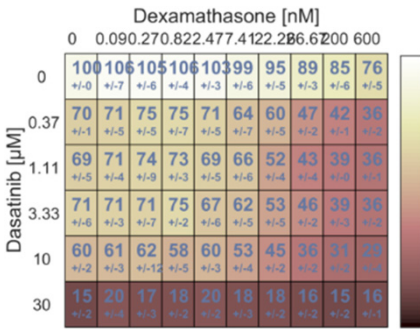
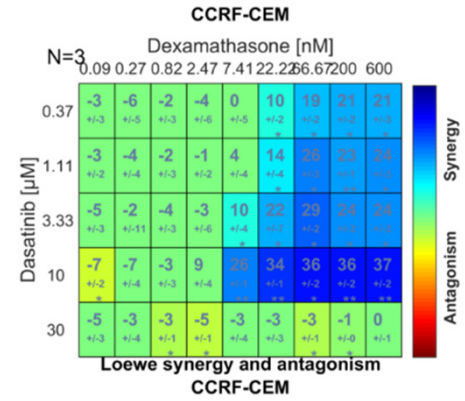
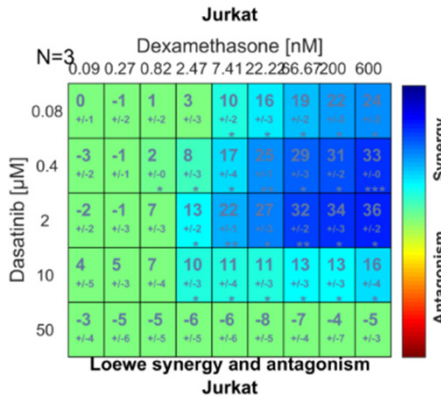
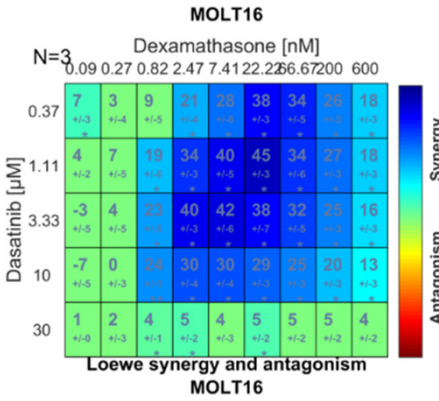
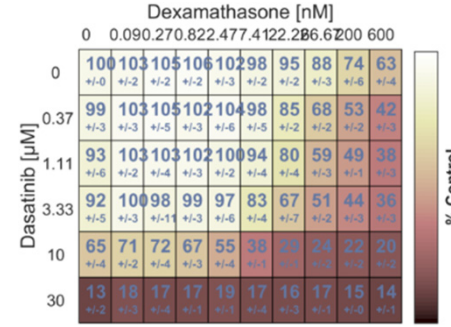
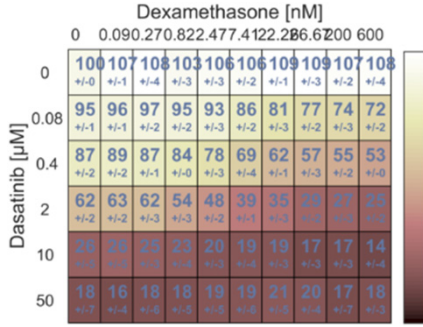
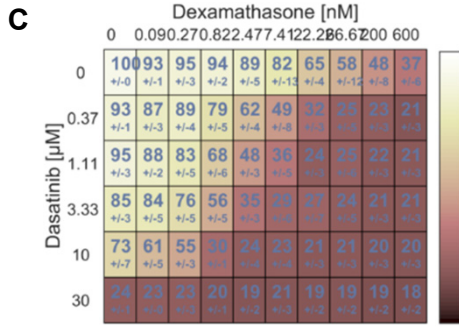
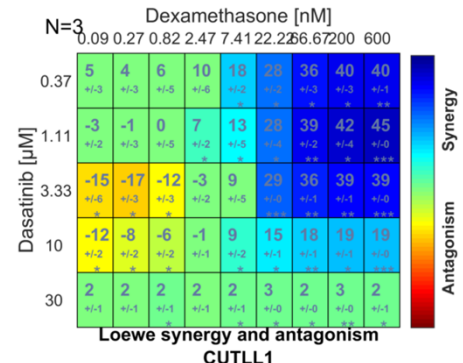
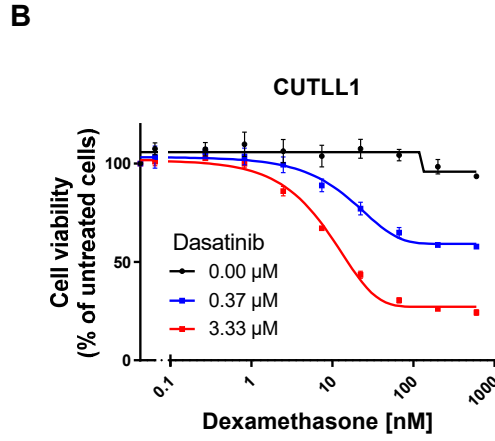
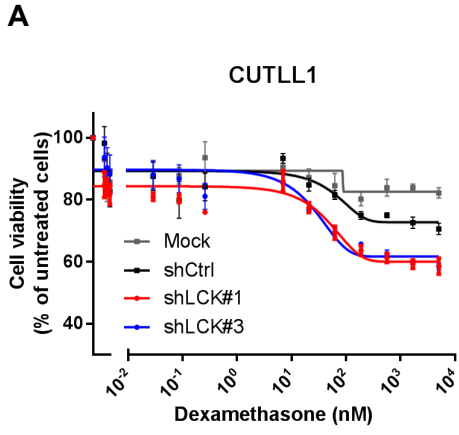
**D**



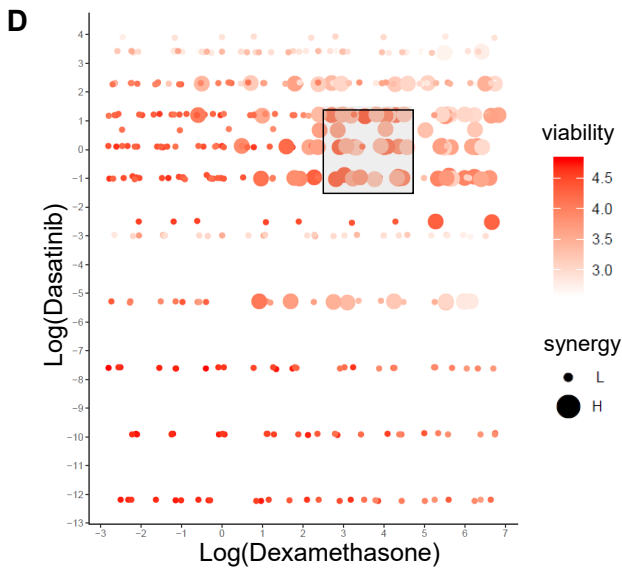
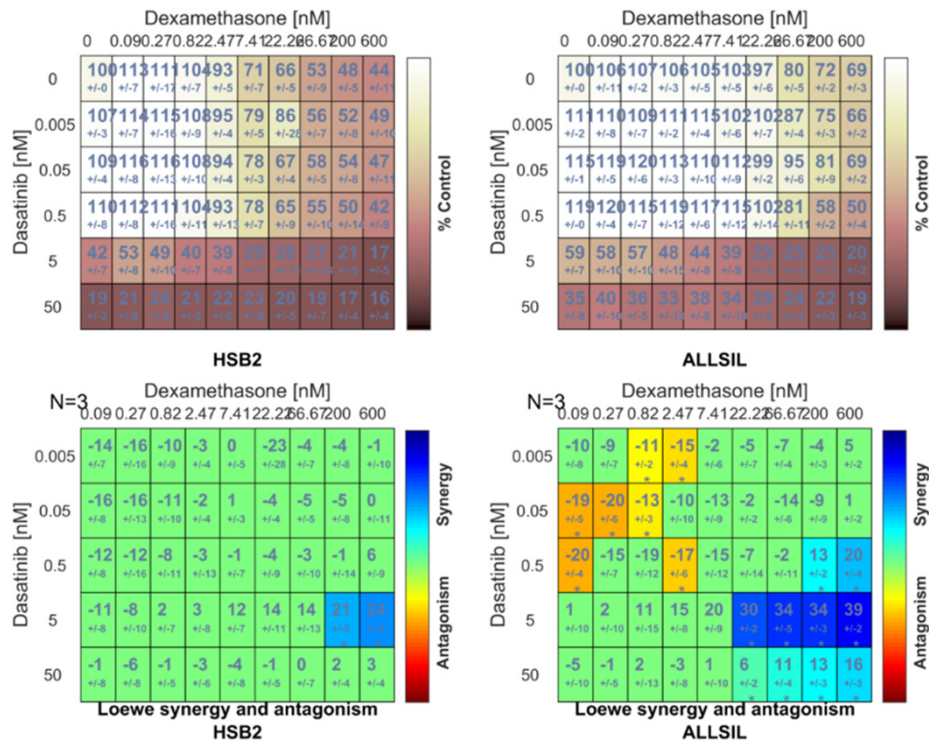
**E**



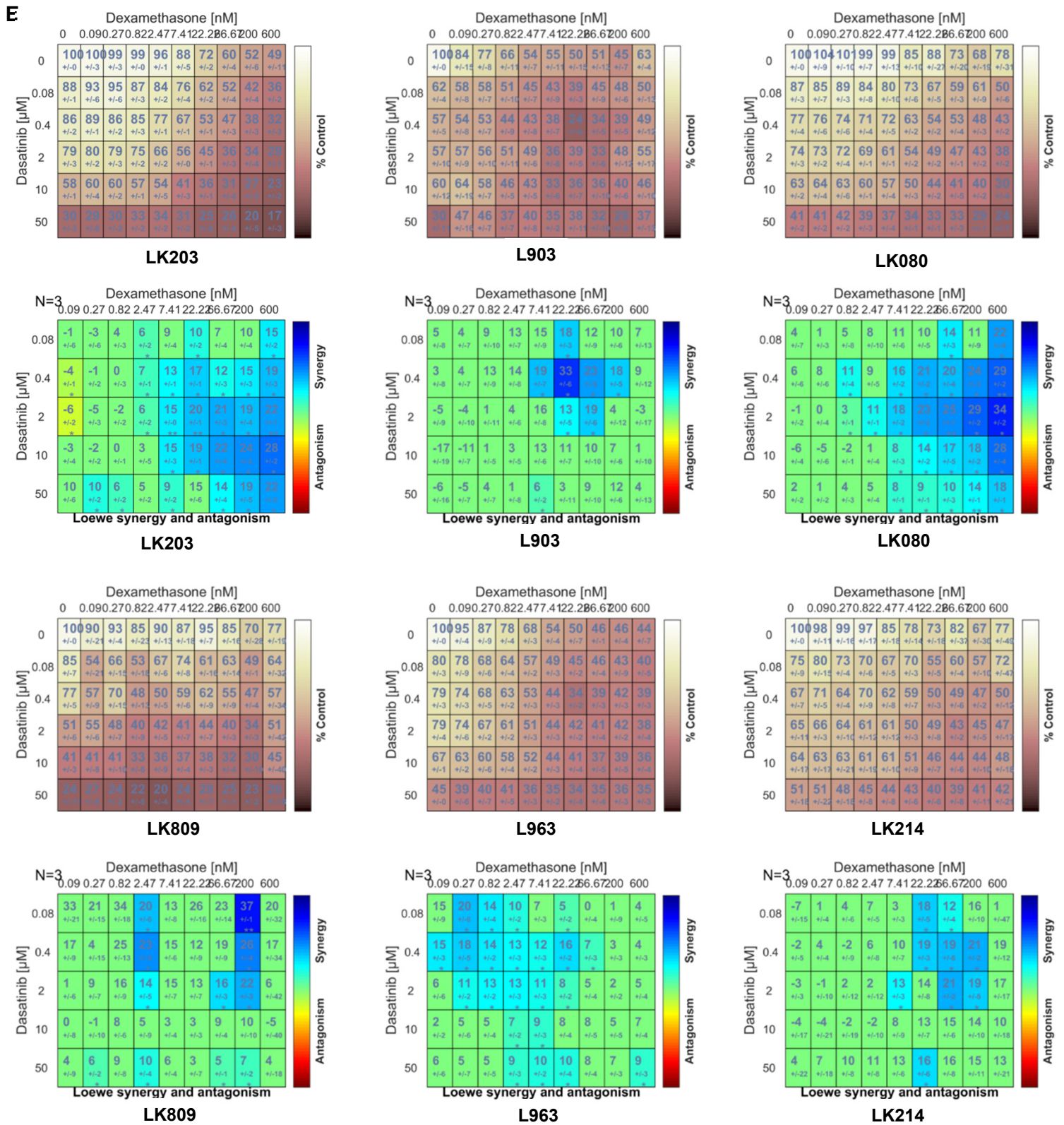
**Supplementary Figure 5. DAS inhibits LCK function and causes cell cycle arrest.** (A-D) Indicated T-ALL cell lines (A, B) or PDX T-ALL (C-D) were treated with vehicle control or DAS (2  $\mu$ M for cell lines, 1  $\mu$ M for PDXs) for 24 h. Phosphorylation of total LCK, p-Y416<sup>SRC</sup>, p-Y505<sup>LCK</sup>, total PLCγ1, p-Y783<sup>PLCγ1</sup>, total ZAP70 and p-Y493<sup>ZAP70</sup> was assessed in Jurkat or CUTLL1 cells (A) and in PDX L970, L907, LK080 and L809 (C) by Western Blot analysis. (B and D) Cell cycle was analysed after Hoechst staining and flow cytometric assessment in various T-ALL cell lines (B) and PDX LK080 (\*\*p=0.0049, n=3) (D). (E) The *in vitro* sensitivity of a panel of PDX samples to DAS ( $GI_{50}$ ) was correlated with the ratio of p-Y416<sup>SRC</sup> / total LCK as determined by Phosflow.



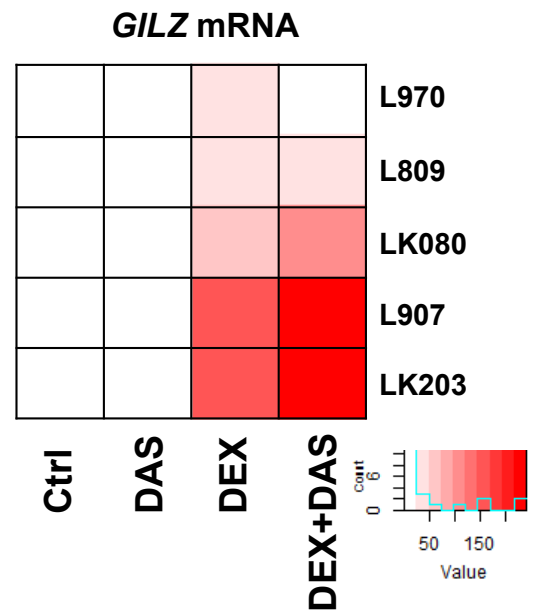
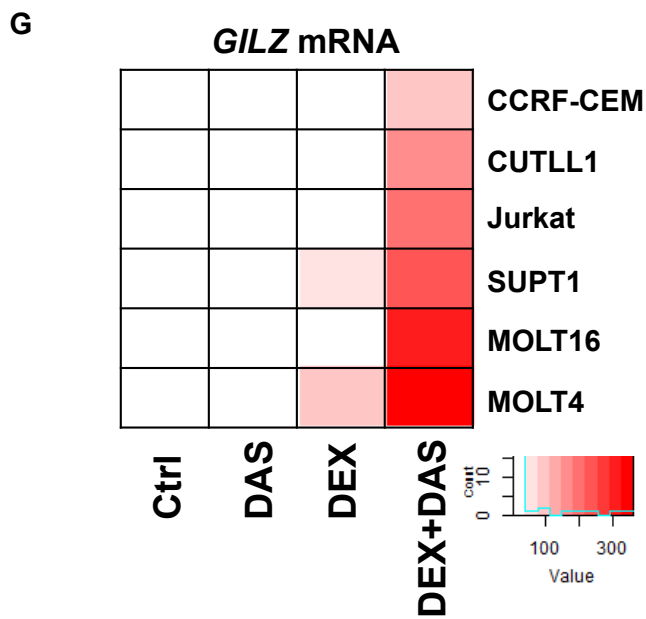
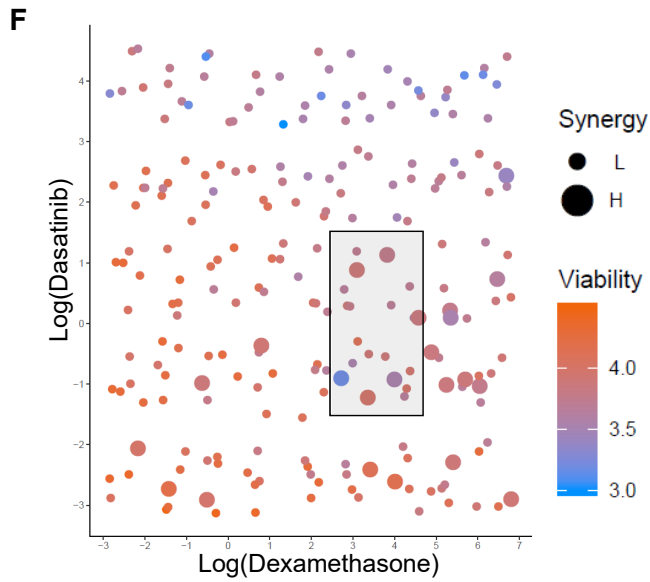




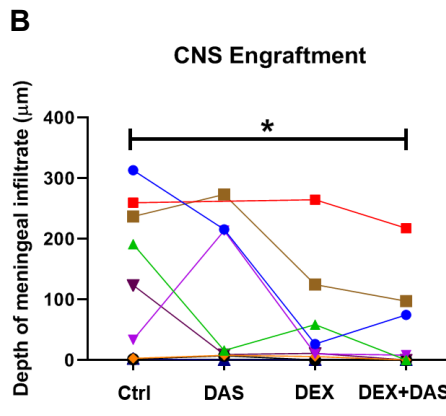
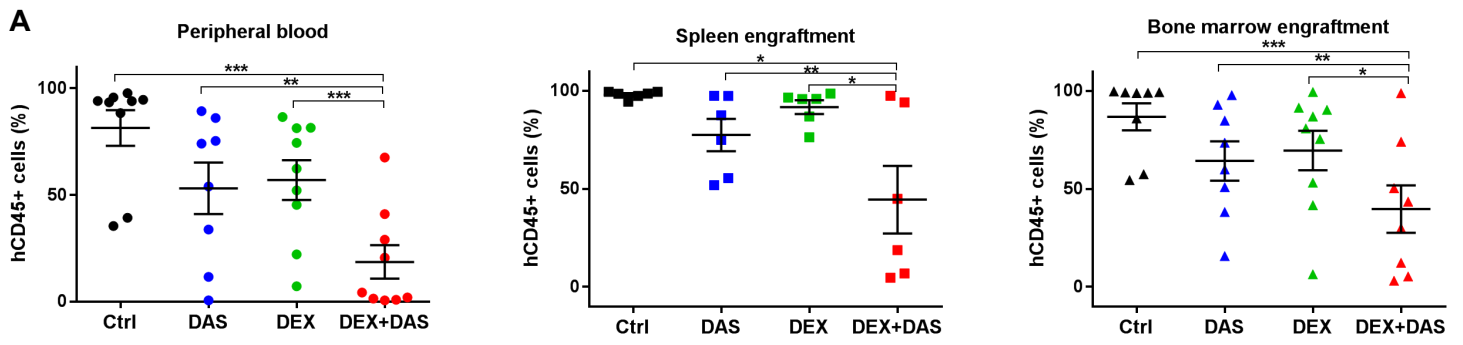
**Supplementary Figure 6. DEX and DAS act synergistically to induce cell death in T-ALL.** (A) Cell viability of parental CUTLL1 cells transduced with (mock), shNTC, shLCK#1 or shLCK#3 upon treatment with increasing DEX concentrations (0-1699 nM). (B-D) Drug matrix analyses with titration of DEX (0-600 nM) and DAS (0.08-50  $\mu$ M) for 72 h was performed in 10 T-ALL cell lines. (B, left) Cell viability of CUTLL1 with and without DAS (black line, no DAS; blue line, 0.37  $\mu$ M; red line, 3.33  $\mu$ M) in combination with increasing concentrations of DEX (0-600 nM) as derived from the drug matrix. (B, Right) Combeneft analysis of drug matrix demonstrates drug synergy in CUTLL1 cells at clinically relevant drug concentrations. (C) Combeneft analysis of drug matrix demonstrates varying levels of drug synergy in T-ALL cell lines. The brown shaded matrices reflect the percentage of viable cell after drug treatment relative to the percentage of viable cells under control conditions. (D) Bioinformatic analysis of all 10 T-ALL cell lines revealed a statistically significant enrichment of drug synergy at clinically relevant concentrations (shaded area). This synergy was observed at 8-110 nM of DEX and 0.223-4.5  $\mu$ M of DAS. Each circle represents one measurement in the drug matrices of 10 cell lines. Circle color represents cell viability. Circle size represents level of synergy calculated.



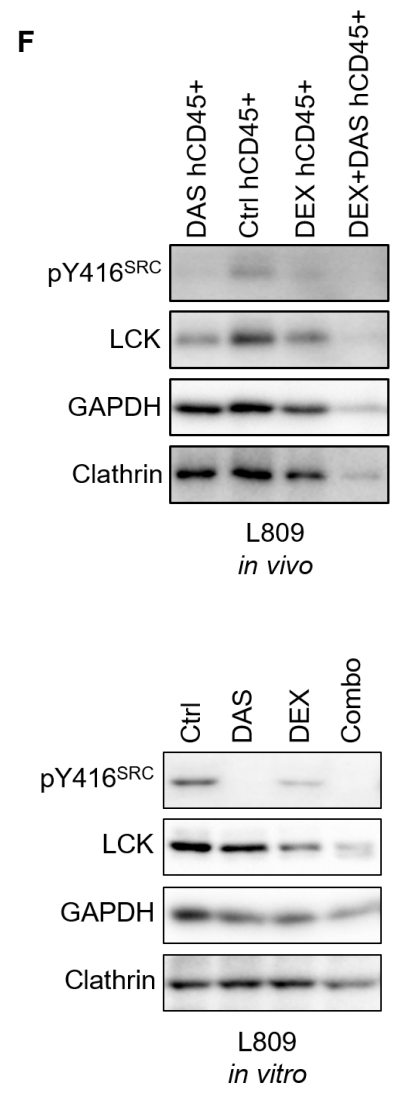
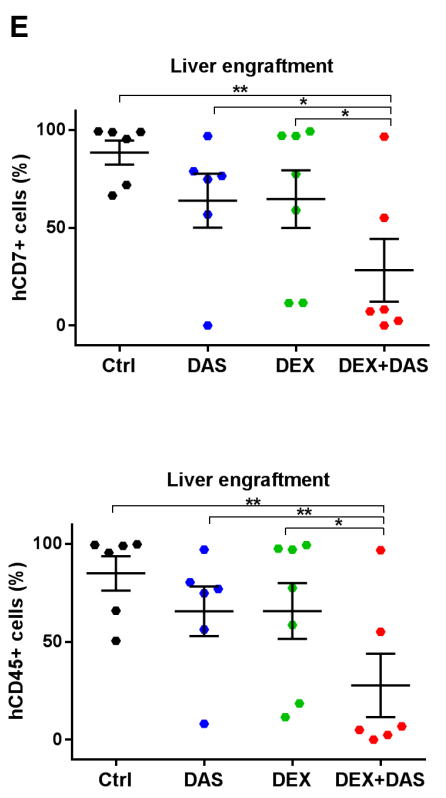
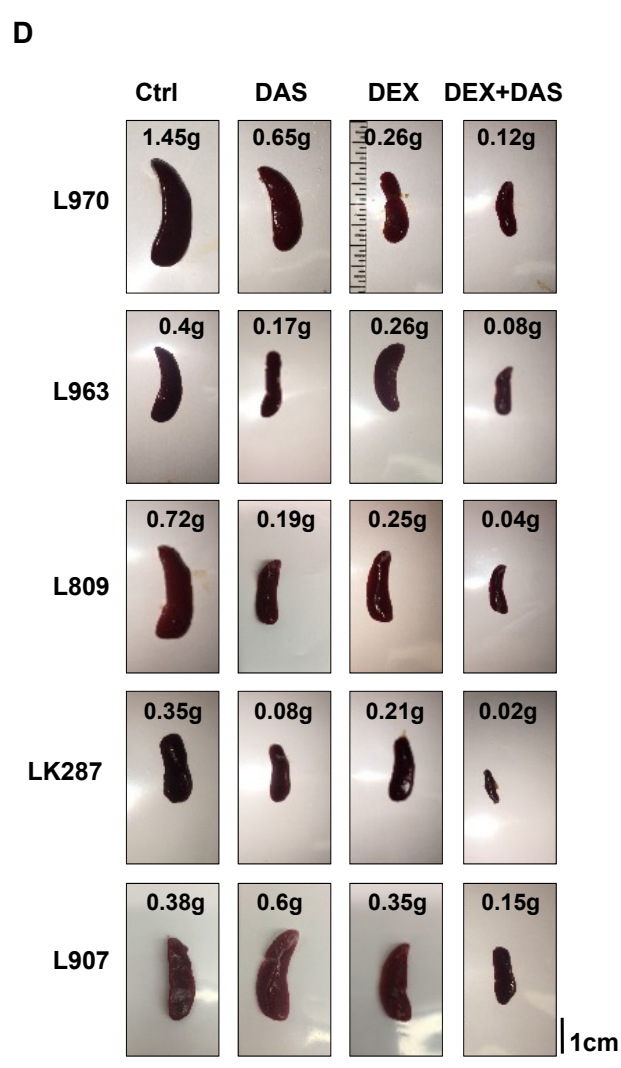
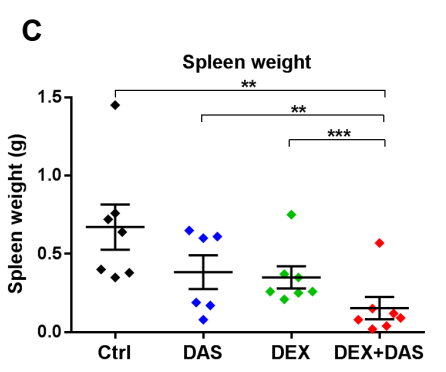
**Supplementary Figure 6.** (E) Combeneft analysis of drug matrices demonstrates varying levels of drug synergy in T-ALL PDX samples. The brown shaded matrices reflect cell viability (%) after drug treatment relative to the cell viability determined under control conditions.



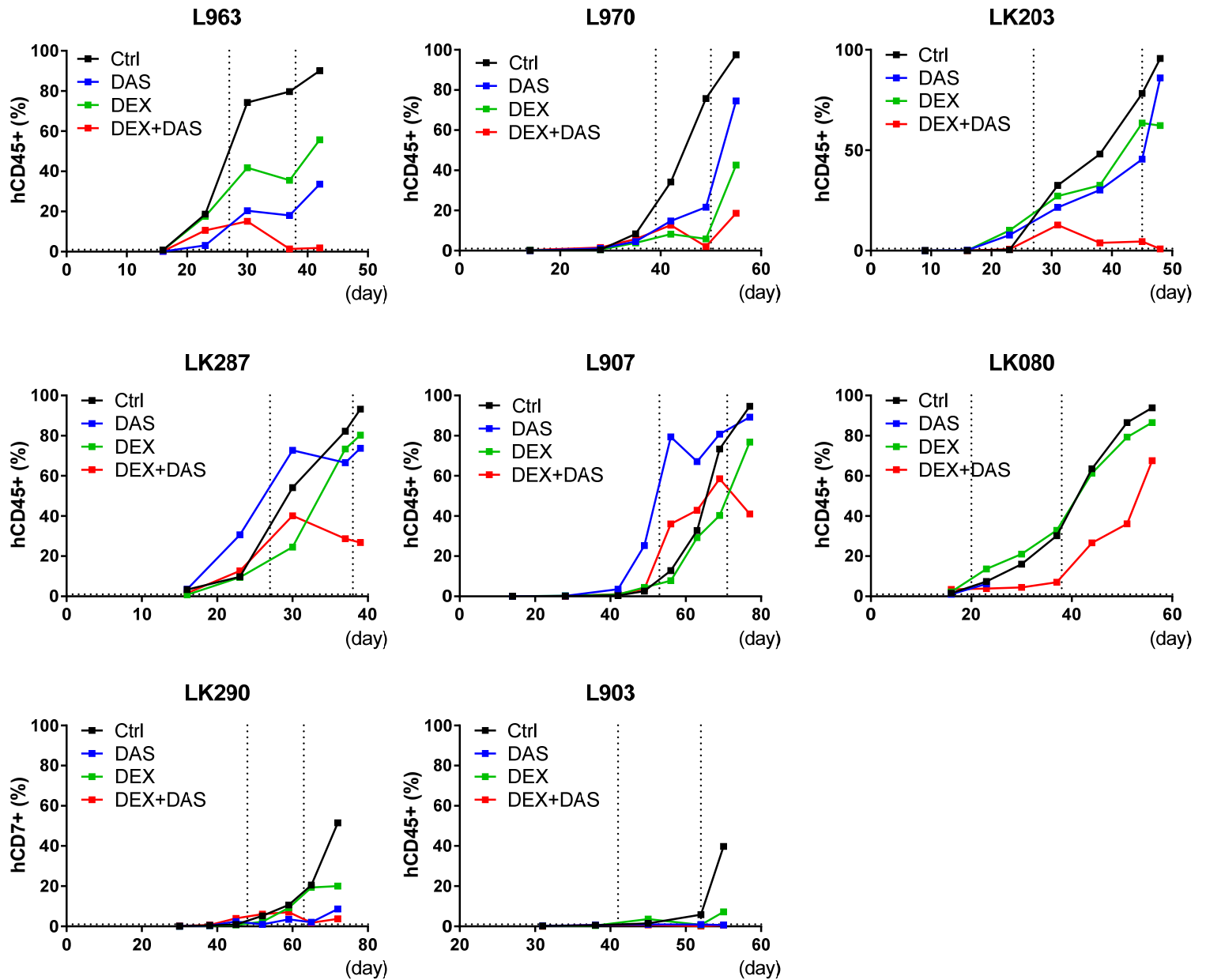
**Supplementary Figure 6.** (F) Bioinformatic analysis of drug matrices/Combeneft analyses of all PDX samples revealed a statistically significant enrichment of drug synergy at clinically relevant concentrations (shaded area). This synergy was observed at 8-110 nM of DEX and 0.223-4.5  $\mu$ M of DAS. Circle color represents cell viability. Circle size represents level of synergy calculated. (G) Real time qPCR analysis of *GILZ* mRNA expression in the cell lines CCRF-CEM, CUTLL1, Jurkat, SUPT1, MOLT16, MOLT4, PDX L970, L809, LK080, L907 and LK203 after exposure to control (Ctrl) conditions, DAS (2  $\mu$ M for cell lines and 1  $\mu$ M for PDXs), DEX (100 nM) or DAS+DEX combination treatment at the same concentrations for 24 h. *GILZ* mRNA expression was normalized to *GAPDH* mRNA expression. Red shading of boxes represent *GILZ* expression relative to control condition.



	Ctrl	DAS	DEX	DEX + DAS
L970	313.2	215.4	26.6	74.4
LK080	259.4	n/a	264.6	217.6
L809	191.2	15.8	58.4	0
L907	33.6	213.6	10.2	8
LK287	2.8	7.8	5.8	0
LK290	1.6	7.2	0	0
LK203	236.8	273	124.6	97
L903	2	0	0	0
L963	123.6	9	11.2	0



G



**Supplementary Figure 7. DEX + DAS synergize to impair leukemia engraftment in a phase II-like murine trial.**

(A) Summary of final human CD45+ engraftment (%) in peripheral blood (left), spleen (middle) and bone marrow (right) of mice treated with Ctrl (black), DAS (blue), DEX (green) or DEX+DAS (red). Paired student t-test was used. Peripheral blood: Ctrl vs DEX+DAS \*\*\* $p < 0.00001$ , DAS vs DEX+DAS \*\* $p = 0.00126$ , DEX vs DEX+DAS \*\*\* $p = 0.00032$ . Spleen: Ctrl vs DEX+DAS \* $p = 0.01068$ , DAS vs DEX+DAS \*\* $p = 0.004259$ , DEX vs DEX+DAS \* $p = 0.01425$ . Bone marrow: Ctrl vs DEX+DAS \*\*\* $p = 0.0003$ , DAS vs DEX+DAS \*\* $p = 0.0056$ , DEX vs DEX+DAS \* $p = 0.01579$ . (B) Average depth of CNS infiltrate across 5 coronal sections per mouse analyzed by paired t-test, significance level \* $p < 0.05$ . Table. Individual values for average depth of infiltrate across 5 sections measured in  $\mu\text{m}$  for each patient sample in the phase II-like trial. (C) Summary of spleen weight in mice treated with Ctrl (black), DAS (blue), DEX (green) or DEX+DAS (red). Paired student t-test was used. Ctrl vs DEX+DAS \*\* $p = 0.002996$ , DAS vs DEX+DAS \*\* $p = 0.006699$ , DEX vs DEX+DAS \*\*\* $p < 0.00001$ . (D) Spleen size and weight in mice derived from 5 PDX samples treated with Ctrl, DAS, DEX or DEX+DAS. (E) Summary of final human CD7+ or CD45+ engraftment (%) in liver of mice treated with Ctrl (black), DAS (blue), DEX (green) or DEX+DAS (red). Paired student t-test was used. Top: Ctrl vs DEX+DAS \*\* $p = 0.001248$ , DAS vs DEX+DAS \* $p = 0.01155$ , DEX vs DEX+DAS \* $p = 0.03188$ . Bottom: Ctrl vs DEX+DAS \*\* $p = 0.002323$ , DAS vs DEX+DAS \*\* $p = 0.00503$ , DEX vs DEX+DAS \* $p = 0.02264$ . (F) Western blotting of total and phosphorylated LCK (p-Y416<sup>SRC</sup>) protein levels of flow sorted hCD45+ cell lysates derived from the spleens of 4 mice injected with PDX L809 under 4 different treatment arms (Ctrl, DAS, DEX or DEX+DAS) relative to the housekeepers GAPDH and Clathrin (top). Western blotting of total and phosphorylated LCK protein levels of whole cell lysates of PDX L809 cells (97% purity) treated *in vitro* for 24 hours with Ctrl, DAS (1  $\mu\text{M}$ ), DEX (100 nM) or DEX+DAS, relative to the housekeepers GAPDH and Clathrin. (G) Engraftment of hCD45+ cells (%) was determined weekly in peripheral blood derived from mice injected with PDX samples. Engraftment levels are shown starting from day of injection (day 0) in mice receiving control vehicle (Ctrl, black), DAS (blue), DEX (green) or DEX+DAS (red). The vertical dotted lines indicate the treatment window.

**Supplementary Figure 1A. Relative gene expression of targets in the shRNA screen.** *In silico* analysis, using the Cancer Cell Line Encyclopedia (CCLE), of gene expression of *LCK*, *FYN*, *ZAP70*, *PTCRA*, *LAT* and *CD3E* in a panel of cancer cell lines.

**Supplementary Figure 1B. Relative gene expression of *LCK* and *PTCRA* in a panel of cell lines and PDX samples.** *LCK* and *pTCRA* expression was determined in various T-ALL cell lines, 697 and REH (B-lineage ALL cell lines) and TK6 (lymphoblastoid cell line) by real time qPCR. *GAPDH* served as reference gene for normalization.

**Supplementary Figure 1C-F. Gradual depletion of shLCK#3 in T-ALL cell lines and PDX LK203 *ex vivo*.** Cells were lentivirally transduced with the pLKO5-shRNA library and the abundance of shRNAs were determined after 40 days (T-ALL cell lines) and 30 days (PDX LK203) growth *ex vivo* (C) Volcano plots representing the change in shRNA representation over time (slope, x-axis) with negative values representing depletion. The y-axis represents the significance in enrichment or depletion of shRNA constructs (log<sub>10</sub> scale). Each dot represents an individual shRNA construct. Dots above the blue line have significantly changed ( $p < 0.05$ ). (D) Heatmap depicting relative representation of shRNA constructs after *in vitro* culture of 4 T-ALL cell lines (40 days). (E) Change in shRNA representation (logCPM) over time (days) for NTC (red, green), *LCK* and *ZAP70* (lib 1 blue, lib 2 purple). shRNA derived from library 1 or 2. (F) Volcano plot representing the magnitude of the fold change (log<sub>2</sub>) in shRNA abundance derived from PDX LK203 leukemia cells on the x-axis. Each dot represents an individual shRNA construct. The y-axis represents the significance in enrichment or depletion of shRNA constructs (log<sub>10</sub> scale). Dots above the blue line are significantly depleted ( $p < 0.05$ ).

**Supplementary Figure 1G. *LCK* protein expression in T-ALL.** Western Blot analysis of *LCK* and p-Y416<sup>SRC</sup> protein expression in a panel of cell lines (left) and PDX samples (right). Comparative expression of housekeepers *GAPDH* and *Clathrin* is shown.

**Supplementary Figure 2. Competitive assays underline a critical role for *LCK* in T-ALL cell proliferation.** (A) T-ALL cell line CUTLL1 was transduced with GFP expressing shLCK (blue), shZAP70 (purple), shPTCRA (red) or shNTC (black; RUNX1/ETO, FLG, NTC) expressing constructs. The cells were seeded in a 1:1 ratio with non-transduced parental cells *in vitro*. Cells were cultured and analyzed repetitively for the presence of GFP+ cells over a time period of 40 days. A relative GFP expression of 1 denotes a mixture of 50% GFP+ cells with 50% parental cells (ratio 1:1). A value of 0.5 means GFP+ cells represent 25% of total cells (ratio 1:4). Three separate shRNAs (#1,2,3) were used to target *LCK*, *PTCRA* and *ZAP70*. The knockdown efficiency at mRNA level is indicated in black bars on the right side of each proliferation plot. (B) CUTLL1 and MOLT4 cells were transduced with GFP expressing shFYN (pink) or shNTC (black) constructs and seeded in a 1:1 ratio with non-transduced parental cells *in vitro*. Cells were cultured and analyzed repetitively for the presence of GFP+ cells over a time period of 40 days. The knockdown efficiency at mRNA level is indicated in black bars on the right side of each proliferation plot. (C)

MOLT4 cells were lentivirally transduced with shNTC (non-targeting control), shLCK#3 (blue), shPTCRA#1 (red), or shZAP70#1 (purple) expression constructs and seeded in a 1:1 ratio with non-transduced parental cells *in vitro*. Cells were cultured and analyzed repetitively by flow cytometry for the presence of GFP+ cells over a time period of 40 days.

**Supplementary Figure 3. Targeted shRNA screen identifies critical role for LCK in T-ALL progression in immunocompromised NSG mice.** (A) Schematic representation of the *in vivo* targeted shRNA screen. (B) Volcano plot representing the magnitude of the fold change (log<sub>2</sub>) in shRNA abundance in PDX L963 bone marrow on the x-axis. shLCK#3 (red dot) represents the shRNA construct with most significant depletion in bone marrow. Bar plot of the normalized shLCK#1 sequencing reads (log<sub>2</sub>) in leukemic cells derived from the bone marrow (orange) or spleen (blue) of 6 individual mice (M1-6), relative to the frequency of these reads before transplantation (green, base line B1-3). (C) Flow cytometric analysis of representation of shNTC (red fluorescent protein, RFP) or shLCK#3 (GFP) constructs in MOLT4 *in vivo* competitive outgrowth assay. MOLT4 cells were derived from splenic tissue.

**Supplementary Figure 4. LCK knockdown results in cell cycle arrest.** (A) Cell cycle status was determined by flow cytometry using Hoechst 33342 in Jurkat and MOLT4 cell lines. (B) Relative S phase ratio in PDX L963 after transduction with shLCK#3 versus shNTC. (C) PDX LK203 and L963 cells were electroporated with siRNA directed against LCK or NTC (Ctrl). Phosflow analysis after 8 days identified reduction in p-Y416<sup>SRC</sup> and total LCK, leading to significant cell cycle arrest in LK203 (\*\*p=0.004, n=3). (E) Flow cytometric analysis of T-ALL cells stained with PE-Annexin V/7-AAD after knockdown with shNTC or shLCK#3. Annexin V positivity, as indicator of early apoptosis, is indicated on the y-axis.

**Supplementary Figure 5. DAS inhibits LCK function and causes cell cycle arrest.** (A-D) Indicated T-ALL cell lines (A, B) or PDX T-ALL (C-D) were treated with vehicle control or DAS (2 μM for cell lines, 1 μM for PDXs) for 24 h. Phosphorylation of total LCK, p-Y416<sup>SRC</sup>, p-Y505<sup>LCK</sup>, total PLCγ1, p-Y783<sup>PLCγ1</sup>, total ZAP70 and p-Y493<sup>ZAP70</sup> was assessed in Jurkat or CUTLL1 cells (A) and in PDX L970, L907, LK080 and L809 (C) by Western Blot analysis. (B and D) Cell cycle was analysed after Hoechst staining and flow cytometric assessment in various T-ALL cell lines (B) and PDX LK080 (\*\*p=0.0049, n=3) (D). (E) The *in vitro* sensitivity of a panel of PDX samples to DAS (GI<sub>50</sub>) was correlated with the ratio of p-Y416<sup>SRC</sup> / total LCK as determined by Phosflow.

**Supplementary Figure 6. DEX and DAS act synergistically to induce cell death in T-ALL.** (A) Cell viability of parental CUTLL1 cells transduced with (mock), shNTC, shLCK#1 or shLCK#3 upon treatment with increasing DEX concentrations (0-1699 nM). (B-F) Drug matrix analyses with titration of DEX (0-600 nM) and DAS (0.08-50 μM) for 72 h was performed in 10 T-ALL cell lines. (B, left) Cell viability of CUTLL1 with and without DAS (black line, no DAS; blue line, 0.37 μM; red line, 3.33 μM) in combination with increasing concentrations of DEX (0-600 nM) as derived from the drug matrix. (B, Right) Combobenefit analysis of drug matrix demonstrates drug synergy

in CUTLL1 cells at clinically relevant drug concentrations. (C) Combenefit analysis of drug matrix demonstrates varying levels of drug synergy in T-ALL cell lines. The brown shaded matrices reflect the percentage of viable cell after drug treatment relative to the percentage of viable cells under control conditions. (D) Bioinformatic analysis of all 10 T-ALL cell lines revealed a statistically significant enrichment of drug synergy at clinically relevant concentrations (shaded area). This synergy was observed at 8-110 nM of DEX and 0.223-4.5  $\mu$ M of DAS. Each circle represents one measurement in the drug matrices of 10 cell lines. Circle color represents cell viability. Circle size represents level of synergy calculated.

**Supplementary Figure 6.** (E) Combenefit analysis of drug matrices demonstrates varying levels of drug synergy in T-ALL PDX samples. The brown shaded matrices reflect cell viability (%) after drug treatment relative to the cell viability determined under control conditions.

**Supplementary Figure 6.** (F) Bioinformatic analysis of drug matrices/Combeneft analyses of all PDX samples revealed a statistically significant enrichment of drug synergy at clinically relevant concentrations (shaded area). This synergy was observed at 8-110 nM of DEX and 0.223-4.5  $\mu$ M of DAS. Circle color represents cell viability. Circle size represents level of synergy calculated. (G) Real time qPCR analysis of *GILZ* mRNA expression in the cell lines CCRF-CEM, CUTLL1, Jurkat, SUPT1, MOLT16, MOLT4, PDX L970, L809, LK080, L907 and LK203 after exposure to control (Ctrl) conditions, DAS (2  $\mu$ M for cell lines and 1  $\mu$ M for PDXs), DEX (100 nM) or DAS+DEX combination treatment at the same concentrations for 24 h. *GILZ* mRNA expression was normalized to *GAPDH* mRNA expression. Red shading of boxes represent *GILZ* expression relative to control condition.

**Supplementary Figure 7. DEX + DAS synergize to impair leukemia engraftment in a phase II-like murine trial.** (A) Summary of final human CD45+ engraftment (%) in peripheral blood (left), spleen (middle) and bone marrow (right) of mice treated with Ctrl (black), DAS (blue), DEX (green) or DEX+DAS (red). Paired student t-test was used. Peripheral blood: Ctrl vs DEX+DAS \*\*\* $p < 0.00001$ , DAS vs DEX+DAS \*\* $p = 0.00126$ , DEX vs DEX+DAS \*\*\* $p = 0.00032$ . Spleen: Ctrl vs DEX+DAS \* $p = 0.01068$ , DAS vs DEX+DAS \*\* $p = 0.004259$ , DEX vs DEX+DAS \* $p = 0.01425$ . Bone marrow: Ctrl vs DEX+DAS \*\*\* $p = 0.0003$ , DAS vs DEX+DAS \*\* $p = 0.0056$ , DEX vs DEX+DAS \* $p = 0.01579$ . (B) Average depth of CNS infiltrate across 5 coronal sections per mouse analyzed by paired t-test, significance level \* $p < 0.05$ . Table. Individual values for average depth of infiltrate across 5 sections measured in  $\mu$ m for each patient sample in the phase II-like trial. (C) Summary of spleen weight in mice treated with Ctrl (black), DAS (blue), DEX (green) or DEX+DAS (red). Paired student t-test was used. Ctrl vs DEX+DAS \*\* $p = 0.002996$ , DAS vs DEX+DAS \*\* $p = 0.006699$ , DEX vs DEX+DAS \*\*\* $p < 0.00001$ . (D) Spleen size and weight in mice derived from 5 PDX samples treated with Ctrl, DAS, DEX or DEX+DAS. (E) Summary of final human CD7+ or CD45+ engraftment (%) in liver of mice treated with Ctrl (black), DAS (blue), DEX (green) or DEX+DAS (red). Paired student t-test was used. Top: Ctrl vs DEX+DAS \*\* $p = 0.001248$ , DAS vs DEX+DAS \* $p = 0.01155$ , DEX vs DEX+DAS \* $p = 0.03188$ . Bottom: Ctrl vs DEX+DAS \*\* $p = 0.002323$ , DAS vs DEX+DAS \*\* $p = 0.00503$ , DEX vs DEX+DAS \* $p = 0.02264$ . (F) Western blotting of total and phosphorylated LCK (p-Y416<sup>SRC</sup>) protein



levels of flow sorted hCD45+ cell lysates derived from the spleens of 4 mice injected with PDX L809 under 4 different treatment arms (Ctrl, DAS, DEX or DEX+DAS) relative to the housekeepers GAPDH and Clathrin (top). Western blotting of total and phosphorylated LCK protein levels of whole cell lysates of PDX L809 cells (97% purity) treated *in vitro* for 24 hours with Ctrl, DAS (1  $\mu$ M), DEX (100 nM) or DEX+DAS, relative to the housekeepers GAPDH and Clathrin. (G) Engraftment of hCD45+ cells (%) was determined weekly in peripheral blood derived from mice injected with PDX samples. Engraftment levels are shown starting from day of injection (day 0) in mice receiving control vehicle (Ctrl, black), DAS (blue), DEX (green) or DEX+DAS (red). The vertical dotted lines indicate the treatment window.

Supplementary Table 1. Sequences of shRNAs used in targeted screen.

Gene	Oligo Sequences
1F	shFYN#1 AGCGACCGATTGATAGAAGACAATGATAGTGAAGCCACAGATGATCATTTGCTTCTATCAATCGGG
1R	GGCACCCGGATTGATAGAAGACAATGATACATCTGTGGCTTCACTATCATTGCTTCTATCAATCGGT
2F	sh#FYN2 AGCGAAGACAATGAGTACACAGCAATAGTGAAGCCACAGATGATTGCTGTACTCATTGCTTCC
2R	GGCAGAAACAATGAGTACACAGCAATACATCTGTGGCTTCACTATTGCTGTACTCATTGCTTCC
3F	shFYN#3 AGCGAATAGAGATCTGCGATCAGCAATAGTGAAGCCACAGATGATTGCTGTACTCAGATCTCTATG
3R	GGCACATAGAGATCTGCGATCAGCAATACATCTGTGGCTTCACTATTGCTGTACTCAGATCTCTATT
4F	shLCK#1 AGCGACGGAATTATATTCATCGTACTAGTGAAGCCACAGATGATGACGATGAATATAATCCGC
4R	GGCAGCGGAATTATATTCATCGTACTACATCTGTGGCTTCACTAGTACGATGAATATAATCCGT
5F	shLCK#2 AGCGACACATGTCTGTACATGTGTATAGTGAAGCCACAGATGATACACATGTACAAGACATGTGC
5R	GGCAGCACATGTCTGTACATGTGTATACATCTGTGGCTTCACTATACACATGTACAAGACATGTGT
6F	shLCK#3 AGCGACCCATCTACATCATCTGAATAGTGAAGCCACAGATGATTCACTGATGATGATAGTGGGC
6R	GGCAGCCATCTACATCATCTGAATACATCTGTGGCTTCACTATTCACTGATGATGATAGTGGGT
7F	shPTCRA#1 AGCGCGCAGATGACTGAGAACAATTAAGTGAAGCCACAGATGATTAATGTTCTCAGTCACTGCT
7R	GGCAGCAGATGACTGAGAACAATAACATCTGTGGCTTCACTAATTAATGTTCTCAGTCACTGCT
8F	shPTCRA#2 AGCGACAGCACAGGCTGTGTCTCAATAGTGAAGCCACAGATGATTGAGCACCAGCCCTGTGCTGG
8R	GGCACCAGCACAGGCTGTGTCTCAATACATCTGTGGCTTCACTATTGAGCACCAGCCCTGTGCTGT
9F	shPTCRA#3 AGCGCAGGGCTTACCTCAGCAGTTATAGTGAAGCCACAGATGATAAAGCTGAGGTAAGACCCCT
9R	GGCAAAGGGCTTACCTCAGCAGTTATACATCTGTGGCTTCACTAATAGCTGAGGTAAGACCCCTG
10F	shZAP70#1 AGCGCGGCGTAGATCACCAGAATAAATAGTGAAGCCACAGATGATTTATCTGGTATCTACGCC
10R	GGCAAGGGCTAGATCACCAGAATAAATACATCTGTGGCTTCACTAATTTATCTGGTATCTACGCCG
11F	shZAP70#2 AGCGAGCCCTGCCCTCATCTATGGGTAGTGAAGCCACAGATGATCCATAGATGAGGGACAGGGCG
11R	GGCAGCCCTGCCCTCATCTATGGGTACATCTGTGGCTTCACTACCCATAGATGAGGGACAGGGCT
12F	shZAP70#3 AGCGCCGCGCAAGGCCCTACAAGAATAGTGAAGCCACAGATGATTCTGTGGGCTTGTGGCCCT
12R	GGCAAGGCCCAAGGCCCTACAAGAATACATCTGTGGCTTCACTATTCTGTAGGGCTTGTGGCCG
13F	shLAT#1 AGCGCCATGGAGTCCATTGATGATTTAGTGAAGCCACAGATGATAATCATCAATGGACTCCATGGA
13R	GGCATCCATGGAGTCCATTGATGATTTACATCTGTGGCTTCACTAATCATCAATGGACTCCATGGG
14F	shLAT#2 AGCGCCAGTGTGGGAGCTACGAGAATAGTGAAGCCACAGATGATTCTCGTAGCTGCCACACCTGT
14R	GGCAACAGTGTGGGAGCTACGAGAATACATCTGTGGCTTCACTATTCTCGTAGCTGCCACACTGT
15F	shLAT#3 AGCGCCCTCAGATAGTTTGTATCAATAGTGAAGCCACAGATGATTGGATACAAACTATCTGAGGA
15R	GGCATCTCAGATAGTTTGTATCAATACATCTGTGGCTTCACTATTGGATACAAACTATCTGAGGG
16F	shCD3E#1 AGCGCACAGAAAGATGCGAACTTTATAGTGAAGCCACAGATGATAAAAGTTCGCATCTTCTGGTT
16R	GGCAAAACAGAAAGATGCGAACTTTATACATCTGTGGCTTCACTAATAAAGTTCGCATCTTCTGGTT
17F	shCD3E#2 AGCGAGGGCAAGATGGTAATGAAGAATAGTGAAGCCACAGATGATTCTCATTACCATTGGCCCG
17R	GGCAGGGCAAGATGGTAATGAAGAATACATCTGTGGCTTCACTATTCTCATTACCATTGGCCCT
18F	shCD3E#3 AGCGACCCCTTCCAGGATATTTATAGTGAAGCCACAGATGATAAATAATCTGGCAAGAGGGC
18R	GGCAGCCCTTCCAGGATATTTATACATCTGTGGCTTCACTAATAAATAATCTGGCAAGAGGGT
19F	shRPL9#1 AGCGGCCCCAGAAAGATGAATTAATCTAGTGAAGCCACAGATGATGATTAATTCATCTTCTGGGCT
19R	GGCAAGCCAGAAAGATGAATTAATCTACATCTGTGGCTTCACTAGATTAATTCATCTTCTGGGCT
20F	shRPL9#2 AGCGAAATTTAGCTTGTTCAAATTTAGTGAAGCCACAGATGATAAATTTGAAACAAGCTCAATGTC
20R	GGCAGACATTTAGCTTGTTCAAATTTACATCTGTGGCTTCACTAATTTGAAACAAGCTCAATGTT
21F	shRPS29#1 AGCGCTCCCTCAGTACCGAAGGATATAGTGAAGCCACAGATGATATCTTCCGCTACTGACGGAA
21R	GGCATTCCCTCAGTACCGAAGGATATACATCTGTGGCTTCACTATATCTTCCGCTACTGACGGAG
22F	shRPS29#2 AGCGACGGCACGGTCTGATCCGGAATAGTGAAGCCACAGATGATTCCGGATCAGACCGTGGCCGG
22R	GGCACGGCACGGTCTGATCCGGAATACATCTGTGGCTTCACTATTCCGGATCAGACCGTGGCCT
23F	shCD19#1 AGCGCGCTCAAGACGCTGGAAGTATTAGTGAAGCCACAGATGATAACTTTCCAGCGTCTTGAGCT
23R	GGCAAGCTCAAGACGCTGGAAGTATTACATCTGTGGCTTCACTAATACTTTCCAGCGTCTTGAGCG
24F	shCD19#2 AGCGCCCCACCAGGATTTCTCAATAGTGAAGCCACAGATGATTGAAGAATCTCTGGTGGGGT
24R	GGCAACCCACCAGGATTTCTCAATACATCTGTGGCTTCACTATTGAAGAATCTCTGGTGGGGG
25F	shTRPM7#1 AGCGGCCCTGACGGTAGATACATTATAGTGAAGCCACAGATGATAATGATATCTACCGTACGGGCT
25R	GGCAAGCCCTGACGGTAGATACATTATACATCTGTGGCTTCACTAATAATGATATCTACCGTACGGGCT
26F	shTRPM7#2 AGCGCGCTGCAGATCTGCTAGCGTATTAGTGAAGCCACAGATGATAACGCTAGCAGATCTGCAGCT
26R	GGCAAGCTGCAGATCTGCTAGCGTATTACATCTGTGGCTTCACTAATACGCTAGCAGATCTGCAGCG
27F	shKLHL7 AGCGCGCAGTTGGCTCTATAGTTTATTAGTGAAGCCACAGATGATAAACTATAGAGCCAAGTCT
27R	GGCAAGCAGTTGGCTCTATAGTTTATTACATCTGTGGCTTCACTAATAAACTATAGAGCCAAGTCT
28F	shDDB2 AGCGAGGAGATATCATGCTCTGGAATTAGTGAAGCCACAGATGATAATCCAGAGCATGATATCTCC
28R	GGCAGGAGATATCATGCTCTGGAATTACATCTGTGGCTTCACTAATCCAGAGCATGATATCTCCT
29F	shSES2 AGCGCGGAGGGATATTAGATTATAATAGTGAAGCCACAGATGATTATAACTAATACTCCCTCCT
29R	GGCAAGGAGGGATATTAGATTATAATACATCTGTGGCTTCACTATTATAACTAATACTCCCTCCT
30F	shERGIC3 AGCGACCTTCAAGAACCAGATACTATAGTGAAGCCACAGATGATAAGTATCTGGGTTCTTGAAGGC
30R	GGCAGCCTTCAAGAACCAGATACTATACATCTGTGGCTTCACTATAGTATCTGGGTTCTTGAAGGT
31F	shFLG AGCGCGGATATAGACCACAACAAGAATAGTGAAGCCACAGATGATTCTTGTGGTCTATATCCA
31R	GGCATGGATATAGACCACAACAAGAATACATCTGTGGCTTCACTATTCTTGTGGTCTATATCCG
32F	shRUNX1/ETO AGCGAAACCTCGAAATCGTACTGAGATAGTGAAGCCACAGATGATCTCAGTACGATTTGAGGTT
32R	GGCAGAACTCGAAATCGTACTGAGATACATCTGTGGCTTCACTATCTCAGTACGATTTGAGGTT
33F	shPTEN#1 AGCGAAGCGCTATGTGATTTATTAGTGAAGCCACAGATGATAAATAACACATAGCGCCT
33R	GGCAGAGCGCTATGTGATTTATTACATCTGTGGCTTCACTAATAATAACACATAGCGCCT
34F	shPTEN#2 AGCGCCACGACGGGAAGCAAGTTCAATAGTGAAGCCACAGATGATAAATGCTTCCCGTCTGT
34R	GGCAACGACGACGGGAAGCAAGTTCAATCTGTGGCTTCACTAATAAATGCTTCCCGTCTGT
35F	shPTEN#3 AGCGACAGCTAAAGGTGAAGATATATAGTGAAGCCACAGATGATAATCTTCACTTTAGCTGGC
35R	GGCAGCCAGCTAAAGGTGAAGATATATACATCTGTGGCTTCACTATATCTTCACTTTAGCTGGT
36F	shNTC AGCGATCTCGTTGGGCGAGATAAGTGAAGCCACAGATGATCTACTCTCGCCAAGCGAGAG
36R	GGCACTCTCGTTGGGCGAGATAAGTACATCTGTGGCTTCACTACTCTCGCCAAGCGAGAT

**Supplementary Table 2. Change in shRNA count over time in CUTLL1.**

shRNA	gene	slope	logCPM	LR	PValue	FDR
shCD19#1	CD19	-0.01426	14.71381	0.229565	0.631846	0.787689
shCD19#2	CD19	0.01455	14.51295	0.233252	0.629123	0.787689
shCD3e#1	CD3e	-0.00759	14.72741	0.066942	0.795843	0.842657
shCD3e#2	CD3e	-0.01372	14.76283	0.225394	0.63496	0.787689
shCD3e#3	CD3e	0.017933	14.88124	0.403658	0.525206	0.787689
shDDB2	DDB2	0.00466	15.3542	0.028696	0.865483	0.865483
shERGIC3	ERGIC3	-0.01392	14.61057	0.229422	0.631952	0.787689
shFLG	FLG	-0.01381	15.7347	0.258837	0.61092	0.787689
shFYN#1	FYN	-0.03403	14.6642	1.363196	0.242984	0.460391
shFYN#2	FYN	-0.03946	14.81744	1.948541	0.162744	0.344635
shFYN#3	FYN	0.021791	14.52647	0.547283	0.45943	0.787594
shKLHL7	KLHL7	0.014446	14.82185	0.258797	0.610948	0.787689
shLAT#1	LAT	0.012082	14.28583	0.142321	0.705985	0.787689
shLAT#2	LAT	0.049563	14.24421	2.267049	0.132151	0.29734
shLAT#3	LAT	0.011454	14.41083	0.137908	0.71037	0.787689
shLCK#1	LCK	-0.05504	14.65581	3.562372	0.059103	0.173345
shLCK#2	LCK	-0.01924	15.03996	0.410081	0.521928	0.787689
shLCK#3	LCK	-0.35675	14.29463	132.3253	1.27E-30	4.57E-29
shNTC	NTC	0.026824	14.92501	0.916581	0.338374	0.609074
shPTCRA#1	PTCRA	0.144236	14.12509	14.74569	0.000123	0.000554
shPTCRA#2	PTCRA	0.04774	14.35548	2.492345	0.114401	0.286763
shPTCRA#3	PTCRA	-0.00638	14.61162	0.044858	0.832265	0.856044
shPTEN#1	PTEN	0.233804	15.29035	71.80669	2.37E-17	2.14E-16
shPTEN#2	PTEN	0.10558	14.9605	12.22175	0.000472	0.001889
shPTEN#3	PTEN	0.270945	14.94674	89.43219	3.17E-21	5.71E-20
shRPL9#1	RPL9	-0.03939	14.58448	1.841226	0.174807	0.349615
shRPL9#2	RPL9	-0.06889	15.13805	5.806092	0.015971	0.052268
shRPS29#1	RPS29	-0.04414	14.94927	2.424066	0.119484	0.286763
shRPS29#2	RPS29	0.287987	13.31127	41.1585	1.40E-10	1.01E-09
shRUNX1/ETC	RUNX1/ETC	0.009921	15.20024	0.126539	0.722048	0.787689
shSESN2	SESN2	0.080821	14.62455	7.360335	0.006668	0.024004
shTRPM7#1	TRPM7	-0.13288	14.8739	18.39057	1.80E-05	9.25E-05
shTRPM7#2	TRPM7	-0.24783	14.66783	74.99375	4.72E-18	5.67E-17
shZAP70#1	ZAP70	-0.14383	14.17178	19.57463	9.67E-06	5.80E-05
shZAP70#2	ZAP70	-0.05783	15.04069	3.467211	0.062597	0.173345
shZAP70#3	ZAP70	0.01156	14.50116	0.149549	0.698967	0.787689

Slope = regression slope

LogCPM = log counts per million

LR = linear regression

Pvalue = calculated probability

FDR = false discovery rate

**Supplementary Table 2. Change in shRNA count over time in HPB-ALL.**

shRNA	gene	slope	logCPM	LR	PValue	FDR
shCD19#1	CD19	-0.02494	14.61324	0.360766	0.548081	0.563741
shCD19#2	CD19	0.322201	14.00891	15.24878	9.42E-05	0.000261
shCD3e#1	CD3e	0.074454	14.68732	0.737249	0.390543	0.438663
shCD3e#2	CD3e	-0.02839	14.99087	0.530497	0.466398	0.493833
shCD3e#3	CD3e	0.110724	14.81066	5.815661	0.015884	0.028591
shDDB2	DDB2	-0.07671	15.54087	4.91949	0.026555	0.043454
shERGIC3	ERGIC3	0.149835	14.66639	8.681668	0.003214	0.00609
shFLG	FLG	-0.03314	15.809	0.840896	0.359141	0.417067
shFYN#1	FYN	-0.1067	14.72682	8.761949	0.003076	0.00609
shFYN#2	FYN	-0.1498	15.14792	10.77279	0.00103	0.002181
shFYN#3	FYN	0.052444	14.53822	1.91671	0.16622	0.213711
shKLHL7	KLHL7	0.094138	14.73021	3.918114	0.047768	0.068787
shLAT#1	LAT	-0.07844	14.33617	4.559337	0.03274	0.04911
shLAT#2	LAT	0.448203	13.41074	82.51448	1.05E-19	9.44E-19
shLAT#3	LAT	-0.08526	14.49881	3.410346	0.064789	0.089708
shLCK#1	LCK	-0.12064	14.80174	10.8718	0.000976	0.002181
shLCK#2	LCK	-0.16964	15.37185	20.91965	4.79E-06	1.57E-05
shLCK#3	LCK	-0.30854	14.80821	71.77447	2.41E-17	1.74E-16
shNTC	NTC	0.142722	14.67407	16.20187	5.69E-05	0.000171
shPTCRA#1	PTCRA	1.162686	12.44823	97.1251	6.51E-23	1.17E-21
shPTCRA#2	PTCRA	-0.09302	14.33642	5.450512	0.019563	0.033536
shPTCRA#3	PTCRA	0.045001	14.68605	1.3185	0.250862	0.301034
shPTEN#1	PTEN	0.192277	15.38286	23.49149	1.25E-06	4.52E-06
shPTEN#2	PTEN	0.360431	15.34098	60.10506	8.99E-15	4.62E-14
shPTEN#3	PTEN	0.324605	15.09946	68.71281	1.14E-16	6.83E-16
shRPL9#1	RPL9	-1.21206	13.30871	93.49248	4.08E-22	4.89E-21
shRPL9#2	RPL9	-0.54714	14.65503	57.88878	2.77E-14	1.25E-13
shRPS29#1	RPS29	-0.1659	15.04966	12.06883	0.000513	0.001231
shRPS29#2	RPS29	1.390155	11.19096	116.9687	2.92E-27	1.05E-25
shRUNX1/ETC	RUNX1/ETC	-0.05371	15.45031	2.394155	0.12179	0.162386
shSESN2	SESN2	0.05198	14.32832	0.702013	0.402108	0.438663
shTRPM7#1	TRPM7	-0.07996	15.19215	4.631726	0.031386	0.04911
shTRPM7#2	TRPM7	-0.01993	14.77305	0.300749	0.583413	0.583413
shZAP70#1	ZAP70	-0.14588	14.20112	12.15537	0.000489	0.001231
shZAP70#2	ZAP70	0.060226	15.03983	1.719252	0.189789	0.235601
shZAP70#3	ZAP70	0.307299	14.0987	40.39811	2.07E-10	8.29E-10

Slope = regression slope

LogCPM = log counts per million

LR = linear regression

Pvalue = calculated probability

FDR = false discovery rate

**Supplementary Table 2. Change in shRNA count over time in MOLT4.**

shRNA	gene	slope	logCPM	LR	PValue	FDR
shCD19#1	CD19	0.076676	14.63632	1.36868	0.242039	0.484078
shCD19#2	CD19	0.304433	14.16582	2.526258	0.111965	0.310058
shCD3e#1	CD3e	0.053084	14.7422	0.320321	0.571415	0.734676
shCD3e#2	CD3e	0.000262	14.94729	1.06E-05	0.997398	0.997398
shCD3e#3	CD3e	0.097748	14.92095	1.407473	0.235476	0.484078
shDDB2	DDB2	-0.01769	15.59403	0.083688	0.77236	0.896935
shERGIC3	ERGIC3	0.1602	14.77733	5.377864	0.020394	0.183544
shFLG	FLG	0.003909	15.84047	0.005994	0.938291	0.965099
shFYN#1	FYN	0.007742	14.81366	0.018907	0.890633	0.948472
shFYN#2	FYN	-0.11644	15.07516	1.8726	0.171178	0.38515
shFYN#3	FYN	0.104816	14.56482	2.537008	0.111205	0.310058
shKLHL7	KLHL7	0.130125	14.88374	4.360828	0.036774	0.231921
shLAT#1	LAT	-0.05618	14.38549	0.709075	0.399751	0.654138
shLAT#2	LAT	0.420649	13.73192	2.350098	0.125275	0.316841
shLAT#3	LAT	-0.0557	14.45989	0.731144	0.392513	0.654138
shLCK#1	LCK	-0.13122	14.76446	4.085409	0.043255	0.231921
shLCK#2	LCK	-0.16797	15.34151	3.129431	0.076891	0.275791
shLCK#3	LCK	-0.49393	14.57817	37.60301	8.67E-10	3.12E-08
shNTC	NTC	0.214847	14.77209	2.980575	0.084269	0.275791
shPTCRA#1	PTCRA	0.267687	12.7532	0.208158	0.648215	0.777858
shPTCRA#2	PTCRA	-0.19116	14.18089	7.283953	0.006957	0.083488
shPTCRA#3	PTCRA	-0.03215	14.61697	0.239374	0.624659	0.775439
shPTEN#1	PTEN	0.030015	15.12332	0.320785	0.571136	0.734676
shPTEN#2	PTEN	0.109527	14.80355	4.015054	0.045096	0.231921
shPTEN#3	PTEN	0.037494	14.68379	0.428577	0.512688	0.734676
shRPL9#1	RPL9	-0.01118	14.45504	0.023847	0.877274	0.948472
shRPL9#2	RPL9	0.007072	15.13202	0.01716	0.895779	0.948472
shRPS29#1	RPS29	-0.32417	14.50428	13.0007	0.000311	0.005605
shRPS29#2	RPS29	0.455703	11.59586	0.554487	0.45649	0.714506
shRUNX1/ETC	RUNX1/ETC	-0.04558	15.46496	0.32547	0.568339	0.734676
shSESN2	SESN2	0.119695	14.52444	2.268625	0.132017	0.316841
shTRPM7#1	TRPM7	-0.04328	15.18369	0.357437	0.549933	0.734676
shTRPM7#2	TRPM7	0.073465	14.78222	0.850954	0.356283	0.641309
shZAP70#1	ZAP70	-0.06882	14.24169	1.04734	0.30612	0.580018
shZAP70#2	ZAP70	0.136615	15.01813	3.505103	0.06118	0.27531
shZAP70#3	ZAP70	0.347658	14.31406	3.121749	0.077254	0.275791

Slope = regression slope

LogCPM = log counts per million

LR = linear regression

Pvalue = calculated probability

FDR = false discovery rate

**Supplementary Table 2. Change in shRNA count over time in SUPT1.**

shRNA	gene	slope	logCPM	LR	PValue	FDR
shCD19#1	CD19	-0.04584	14.65114	0.636513	0.424976	0.546398
shCD19#2	CD19	0.12862	14.4973	5.898472	0.015154	0.030308
shCD3e#1	CD3e	-0.24225	14.39331	19.64187	9.34E-06	3.36E-05
shCD3e#2	CD3e	-0.14202	14.55194	6.734616	0.009456	0.020024
shCD3e#3	CD3e	-0.09928	14.71464	3.841146	0.050009	0.090017
shDDB2	DDB2	0.08035	15.58186	2.732132	0.098348	0.153936
shERGIC3	ERGIC3	0.065503	14.82244	1.627733	0.202017	0.28986
shFLG	FLG	0.018123	15.83752	0.129273	0.719188	0.809086
shFYN#1	FYN	-0.07978	14.72385	2.471572	0.115922	0.173883
shFYN#2	FYN	0.027577	15.02277	0.293038	0.58828	0.705936
shFYN#3	FYN	0.08937	14.62285	2.836867	0.092124	0.150748
shKLHL7	KLHL7	0.162163	15.11518	8.211222	0.004163	0.009367
shLAT#1	LAT	-0.01131	14.34605	0.043935	0.833974	0.857802
shLAT#2	LAT	0.273	14.31746	14.00058	0.000183	0.000598
shLAT#3	LAT	-0.04232	14.63143	0.364078	0.54625	0.678104
shLCK#1	LCK	-0.34628	14.26935	25.45437	4.53E-07	2.04E-06
shLCK#2	LCK	-0.06171	15.14572	1.575962	0.209343	0.28986
shLCK#3	LCK	-0.61735	13.94143	52.16641	5.10E-13	6.12E-12
shNTC	NTC	0.062558	15.05358	1.325919	0.249533	0.33271
shPTCRA#1	PTCRA	-0.07778	12.83142	0.260297	0.609916	0.70829
shPTCRA#2	PTCRA	-0.54271	13.57462	46.17613	1.08E-11	9.73E-11
shPTCRA#3	PTCRA	-0.35518	14.13973	12.15597	0.000489	0.001258
shPTEN#1	PTEN	0.289544	15.57128	20.91663	4.80E-06	1.92E-05
shPTEN#2	PTEN	0.282258	15.35395	35.02909	3.25E-09	2.34E-08
shPTEN#3	PTEN	0.424263	15.38662	32.73342	1.06E-08	6.34E-08
shRPL9#1	RPL9	-0.55786	13.85047	67.01331	2.70E-16	4.85E-15
shRPL9#2	RPL9	-0.18126	14.89238	12.83435	0.00034	0.001021
shRPS29#1	RPS29	-0.53123	14.29437	72.14488	2.00E-17	7.20E-16
shRPS29#2	RPS29	0.628086	12.66522	8.708742	0.003167	0.007601
shRUNX1/ETC	RUNX1/ETC	0.012942	15.29902	0.067097	0.795612	0.842413
shSESN2	SESN2	0.129881	14.83796	5.430274	0.019791	0.037498
shTRPM7#1	TRPM7	-0.00974	15.0676	0.025845	0.87228	0.87228
shTRPM7#2	TRPM7	-0.19066	14.65694	12.51527	0.000404	0.001118
shZAP70#1	ZAP70	-0.37416	13.77377	31.02042	2.55E-08	1.31E-07
shZAP70#2	ZAP70	0.02048	15.15053	0.069517	0.792042	0.842413
shZAP70#3	ZAP70	0.121387	14.66767	3.03661	0.081406	0.139553

Slope = regression slope

LogCPM = log counts per million

LR = linear regression

Pvalue = calculated probability

FDR = false discovery rate

**Supplementary Table 3. Change in shRNA count over time in PDX L963 in vivo BM.**

shRNA	logFC	logCPM	LR	PValue	FDR
shLCK#3	-8.57718	12.38082	26.24361	3.01E-07	1.08E-05
shRPL9#1	-6.49117	11.56515	9.817988	0.001728	0.031106
shCD19#2	-3.25763	12.52308	6.059984	0.013828	0.160969
shERGIC3	4.058343	16.74306	5.607333	0.017885	0.160969
shPTEN#1	-2.94281	16.29354	3.816812	0.050741	0.365333
shPTEN#3	-2.59947	12.77494	3.110715	0.077779	0.390707
shLAT#3	-2.39486	13.02144	3.075171	0.079496	0.390707
shLAT#2	-1.92967	12.92357	2.9323	0.086824	0.390707
shPTCRA#2	1.95272	16.3038	1.774488	0.182828	0.731311
shKLHL7	-1.47015	14.4175	1.514979	0.218381	0.762553
shFYN#1	-1.3497	13.22957	1.422439	0.233002	0.762553
shDDB2	1.461431	16.93928	1.028954	0.310405	0.906671
shCD3E#2	-1.28722	13.91845	0.959119	0.327409	0.906671
shCD3E#3	-1.04132	14.28719	0.636985	0.424805	0.922599
shZAP70#3	1.02018	14.20344	0.618771	0.431504	0.922599
shSESN2	-0.82483	14.09281	0.494419	0.481963	0.922599
shLCK#2	0.795998	15.19829	0.363831	0.546386	0.922599
shRUNX1/ETO	-0.78189	13.95386	0.338049	5.61E-01	9.23E-01
shZAP70#2	-0.53391	14.9653	0.236764	0.626553	0.922599
shTRPM7#1	-0.6809	16.76503	0.20726	0.648923	0.922599
shNTC	0.408758	14.50807	0.155089	0.693718	0.922599
shLCK#1	0.737421	14.11903	0.153269	0.695431	0.922599
shCD19#1	0.678317	15.03059	0.145387	0.702983	0.922599
shZAP70#1	-0.68116	13.5309	0.126603	0.721981	0.922599
shFYN#3	0.510772	14.69092	0.11697	0.732345	0.922599
shRPS29#1	-0.44438	14.52556	0.095859	0.756857	0.922599
shRPL9#2	0.47237	14.19795	0.091172	0.762693	0.922599
shFLG	-0.37716	15.06153	0.081228	0.775641	0.922599
shFYN#2	-0.41495	14.25891	0.079526	0.777941	0.922599
shLAT#1	0.35956	15.05768	0.050328	0.822494	0.922599
shPTCRA#3	-0.26426	13.87086	0.047526	0.827426	0.922599
shTRPM7#2	-0.26199	14.70756	0.03781	0.845825	0.922599
shPTEN#2	-0.24905	14.2727	0.027004	0.869473	0.922599
shPTCRA#1	-0.2584	12.41615	0.026229	0.871343	0.922599
shCD3E#1	0.050404	15.02011	0.001907	0.965171	0.965706
shRPS29#2	0.08799	10.95056	0.001849	0.965706	0.965706

LogFC = log fold change

LogCPM = log counts per million

LR = linear regression

Pvalue = calculated probability

FDR = false discovery rate

**Supplementary Table 3. Change in shRNA count over time in PDX L963 in vivo spleen.**

shRNA	logFC	logCPM	LR	PValue	FDR
shLCK#3	-8.03321	12.38082	31.3336	2.17E-08	7.82E-07
shRPL9#1	-6.10375	11.56515	10.30905	0.001324	0.023828
shCD19#2	-3.204	12.52308	5.983788	0.014438	0.173256
shFYN#1	-1.84535	13.22957	3.100858	0.078251	0.70426
shPTEN#3	-2.03758	12.77494	2.452733	0.11732	0.844707
shERGIC3	2.276879	16.74306	2.167813	0.140927	0.845559
shPTEN#1	-1.68258	16.29354	1.21885	0.269586	0.97833
shZAP70#1	-1.7052	13.5309	1.21095	0.271144	0.97833
shRUNX1/ETO	-1.24494	13.95386	1.073682	0.300115	0.97833
shSESN2	-1.19801	14.09281	0.952131	0.329178	0.97833
shLAT#3	-1.22223	13.02144	0.900891	0.342543	0.97833
shPTCRA#2	1.322231	16.3038	0.800911	0.370821	0.97833
shKLHL7	-1.08219	14.4175	0.763621	0.382198	0.97833
shCD3E#2	-1.11341	13.91845	0.727283	0.393765	0.97833
shLAT#1	1.335508	15.05768	0.68568	0.407638	0.97833
shLAT#2	-0.97306	12.92357	0.572829	0.449137	0.983201
shCD19#1	1.115446	15.03059	0.441655	0.506325	0.983201
shCD3E#3	-0.60982	14.28719	0.219188	0.63966	0.983201
shDDB2	0.588038	16.93928	0.207383	0.648827	0.983201
shFYN#3	0.565636	14.69092	0.16716	0.682649	0.983201
shNTC	0.412178	14.50807	0.165008	0.684587	0.983201
shLCK#1	-0.76202	14.11903	0.157834	0.691159	0.983201
shCD3E#1	-0.43304	15.02011	0.143895	0.704439	0.983201
shFYN#2	-0.49307	14.25891	0.119843	0.729204	0.983201
shFLG	-0.38268	15.06153	0.093593	0.759658	0.983201
shPTCRA#1	-0.34852	12.41615	0.050705	0.821841	0.983201
shTRPM7#1	0.316594	16.76503	0.044782	0.832406	0.983201
shPTCRA#3	-0.23218	13.87086	0.042135	0.837362	0.983201
shZAP70#2	0.20482	14.9653	0.0318	0.858466	0.983201
shTRPM7#2	-0.15276	14.70756	0.012512	0.910937	0.983201
shPTEN#2	0.157617	14.2727	0.011548	0.914423	0.983201
shLCK#2	0.12677	15.19829	0.010496	0.918399	0.983201
shRPL9#2	-0.12975	14.19795	0.008017	0.928657	0.983201
shZAP70#3	0.053671	14.20344	0.001976	0.964547	0.983201
shRPS29#1	0.037446	14.52556	0.000707	0.978787	0.983201
shRPS29#2	-0.04447	10.95056	0.000443	0.983201	0.983201

LogFC = log fold change

LogCPM = log counts per million

LR = linear regression

Pvalue = calculated probability

FDR = false discovery rate



**Supplementary Table 3. Change in shRNA count over time in PDX LK203 ex vivo.**

shRNA	logFC	logCPM	LR	PValue	FDR
shRPL9#2	-2.34442	14.34755	57.47394	3.42E-14	1.23E-12
shRPS29#1	-3.28914	13.91702	18.12502	2.07E-05	0.0003
shSESN2	1.058582	14.68708	17.23154	3.31E-05	0.0003
shERGIC3	1.769788	15.65966	17.22071	3.33E-05	0.0003
shPTEN#3	0.97378	15.07812	15.42601	8.58E-05	0.000618
shLCK#1	-0.77115	14.55244	10.42664	0.001242	0.007453
shLAT#1	-0.79255	14.38541	10.03618	1.53E-03	0.007894
shZAP70#3	0.913031	14.12767	8.893602	0.002862	0.012878
shLCK#2	-0.67921	15.12368	7.527476	0.006076	0.022739
shLAT#3	-0.81492	14.37636	7.457751	0.006316	0.022739
shRPL9#1	-1.72479	13.97955	5.985659	0.014423	0.047201
shLCK#3	-0.65503	15.0903	5.812054	0.015917	0.04775
shPTEN#2	0.577326	15.27768	4.590465	0.03215	0.086249
shTRPM7#2	-0.69319	14.87496	4.517927	0.033541	0.086249
shCD19#2	0.563898	14.21015	3.744642	0.052977	0.122818
shPTEN#1	0.513298	14.97789	3.6947	0.054586	0.122818
shTRPM7#1	0.619672	15.45041	3.558532	0.05924	0.12545
shPTCRA#3	-0.53497	14.5679	3.154093	0.075737	0.151474
shNTC	0.43134	14.77022	2.861392	0.090729	0.171907
shFYN#1	-0.45909	14.66029	2.5511	0.110218	0.198392
shPTCRA#2	-0.94997	14.01477	2.396064	0.121641	0.208527
shCD3E#3	0.350878	14.81547	2.265706	0.132266	0.216245
shFYN#2	-0.36781	15.08274	2.198372	0.138157	0.216245
shCD3E#2	0.363319	15.12521	1.809009	0.178627	0.267941
shPTCRA#1	0.764157	13.1688	1.504773	2.20E-01	0.316711
shCD3E#1	0.284976	14.5903	1.312212	0.251995	0.343891
shRPS29#2	0.792341	10.99167	1.273523	2.59E-01	3.44E-01
shKLHL7	0.278821	14.20479	1.229674	2.67E-01	0.343891
shRUNX1/ETO	-0.26394	15.47563	1.101449	0.293948	0.364901
shDDB2	-0.24191	15.4647	0.99148	0.319381	0.383257
shZAP70#1	-0.2403	14.2102	0.766361	3.81E-01	0.442853
shCD19#1	0.151835	14.9887	0.447914	0.503327	0.566243
shFYN#3	0.134089	14.51175	0.32771	0.567011	0.618557
shLAT#2	0.173499	13.50733	0.187032	0.665398	0.704539
shFLG	0.026086	15.75399	0.011679	0.913942	0.9148
shZAP70#2	-0.02632	15.0016	0.011446	0.9148	0.9148

LogFC = log fold change

LogCPM = log counts per million

LR = linear regression

Pvalue = calculated probability

FDR = false discovery rate

**Supplementary Table 4. Barcode sequences used in library preparation**

<b>Name</b>	<b>Sequences</b>	<b>Primer Seq</b>	<b>Read</b>
1	CAAGCAGAAGACGGCATAACGAGATCGTGATATTTATACCATTTTAATTCAGCTTTGT	CGTGAT	ATCACG
2	CAAGCAGAAGACGGCATAACGAGATACATCGATTTATACCATTTTAATTCAGCTTTGT	ACATCG	CGATGT
3	CAAGCAGAAGACGGCATAACGAGATGCCTAAATTTATACCATTTTAATTCAGCTTTGT	GCCTAA	TTAGGC
4	CAAGCAGAAGACGGCATAACGAGATTGGTCAATTTATACCATTTTAATTCAGCTTTGT	TGGTCA	TGACCA
5	CAAGCAGAAGACGGCATAACGAGATCACTGTATTTATACCATTTTAATTCAGCTTTGT	CACTGT	ACAGTG
6	CAAGCAGAAGACGGCATAACGAGATATTGGCATTTATACCATTTTAATTCAGCTTTGT	ATTGGC	GCCAAT
7	CAAGCAGAAGACGGCATAACGAGATGATCTGATTTATACCATTTTAATTCAGCTTTGT	GATCTG	CAGATC
8	CAAGCAGAAGACGGCATAACGAGATTCAAGTATTTATACCATTTTAATTCAGCTTTGT	TCAAGT	ACTTGA
9	CAAGCAGAAGACGGCATAACGAGATCTGATCATTTTATACCATTTTAATTCAGCTTTGT	CTGATC	GATCAG
10	CAAGCAGAAGACGGCATAACGAGATAAGCTAATTTATACCATTTTAATTCAGCTTTGT	AAGCTA	TAGCTT
11	CAAGCAGAAGACGGCATAACGAGATGTAGCCATTTTATACCATTTTAATTCAGCTTTGT	GTAGCC	GGCTAC
12	CAAGCAGAAGACGGCATAACGAGATTACAAGATTTTATACCATTTTAATTCAGCTTTGT	TACAAG	CTTGTA
13	CAAGCAGAAGACGGCATAACGAGATTTGACTATTTTATACCATTTTAATTCAGCTTTGT	TTGACT	AGTCAA
14	CAAGCAGAAGACGGCATAACGAGATGGAACATTTTATACCATTTTAATTCAGCTTTGT	GGAAC	AGTTCC
15	CAAGCAGAAGACGGCATAACGAGATTGACATATTTTATACCATTTTAATTCAGCTTTGT	TGACAT	ATGTCA
16	CAAGCAGAAGACGGCATAACGAGATGGACGGATTTTATACCATTTTAATTCAGCTTTGT	GGACGG	CCGTCC
17	CAAGCAGAAGACGGCATAACGAGATCTCTACATTTTATACCATTTTAATTCAGCTTTGT	CTCTAC	GTAGAG
18	CAAGCAGAAGACGGCATAACGAGATGCGGACATTTTATACCATTTTAATTCAGCTTTGT	GCGGAC	GTCCGC
19	CAAGCAGAAGACGGCATAACGAGATTTTCACATTTTATACCATTTTAATTCAGCTTTGT	TTTCAC	GTGAAA
20	CAAGCAGAAGACGGCATAACGAGATGTGGCCATTTTATACCATTTTAATTCAGCTTTGT	GTGGCC	GTGGCC
21	CAAGCAGAAGACGGCATAACGAGATCGAAACATTTTATACCATTTTAATTCAGCTTTGT	CGAAAC	GTTTCG
22	CAAGCAGAAGACGGCATAACGAGATCGTACGATTTTATACCATTTTAATTCAGCTTTGT	CGTACG	CGTACG
23	CAAGCAGAAGACGGCATAACGAGATCCACTCATTTTATACCATTTTAATTCAGCTTTGT	CCACTC	GAGTGG
24	CAAGCAGAAGACGGCATAACGAGATGCTACCATTTTATACCATTTTAATTCAGCTTTGT	GCTACC	GGTAGC
25	CAAGCAGAAGACGGCATAACGAGATATCAGTATTTTATACCATTTTAATTCAGCTTTGT	ATCAGT	ACTGAT
26	CAAGCAGAAGACGGCATAACGAGATGCTCATATTTTATACCATTTTAATTCAGCTTTGT	GCTCAT	ATGAGC
27	CAAGCAGAAGACGGCATAACGAGATAGGAATATTTTATACCATTTTAATTCAGCTTTGT	AGGAAT	ATTCCT
28	CAAGCAGAAGACGGCATAACGAGATCTTTTGATTTTATACCATTTTAATTCAGCTTTGT	CTTTTG	CAAAAAG
29	CAAGCAGAAGACGGCATAACGAGATTAGTTGATTTTATACCATTTTAATTCAGCTTTGT	TAGTTG	CAACTA
30	CAAGCAGAAGACGGCATAACGAGATCCGGTGATTTTATACCATTTTAATTCAGCTTTGT	CCGGTG	CACCGG
31	CAAGCAGAAGACGGCATAACGAGATATCGTGATTTTATACCATTTTAATTCAGCTTTGT	ATCGTG	CACGAT

32	CAAGCAGAAGACGGCATAACGAGATTGAGTGATTTATACCATTTTAATTCAGCTTTGT	TGAGTG	CACTCA
33	CAAGCAGAAGACGGCATAACGAGATGCGGACATTTATACCATTTTAATTCAGCTTTGT	GCGGAC	GCGGAC
34	CAAGCAGAAGACGGCATAACGAGATGCCATGATTTATACCATTTTAATTCAGCTTTGT	GCCATG	CATGGC
35	CAAGCAGAAGACGGCATAACGAGATAAAATGATTTATACCATTTTAATTCAGCTTTGT	AAAATG	CATTTT
36	CAAGCAGAAGACGGCATAACGAGATTGTTGGATTTATACCATTTTAATTCAGCTTTGT	TGTTGG	CCAACA
37	CAAGCAGAAGACGGCATAACGAGATATTCCGATTTATACCATTTTAATTCAGCTTTGT	ATTCCG	CGGAAT
38	CAAGCAGAAGACGGCATAACGAGATAGCTAGATTTATACCATTTTAATTCAGCTTTGT	AGCTAG	CTAGCT
39	CAAGCAGAAGACGGCATAACGAGATGTATAGATTTATACCATTTTAATTCAGCTTTGT	GTATAG	CTATAC
40	CAAGCAGAAGACGGCATAACGAGATTCTGAGATTTATACCATTTTAATTCAGCTTTGT	TCTGAG	CTCAGA
41	CAAGCAGAAGACGGCATAACGAGATGTCGTCATTTATACCATTTTAATTCAGCTTTGT	GTCGTC	GACGAC
42	CAAGCAGAAGACGGCATAACGAGATCGATTAATTTATACCATTTTAATTCAGCTTTGT	CGATTA	TAATCG
43	CAAGCAGAAGACGGCATAACGAGATGCTGTAATTTATACCATTTTAATTCAGCTTTGT	GCTGTA	TACAGC
44	CAAGCAGAAGACGGCATAACGAGATATTATAATTTATACCATTTTAATTCAGCTTTGT	ATTATA	TATAAT
45	CAAGCAGAAGACGGCATAACGAGATGAATGAATTTATACCATTTTAATTCAGCTTTGT	GAATGA	TCATTC
46	CAAGCAGAAGACGGCATAACGAGATTCGGGAATTTATACCATTTTAATTCAGCTTTGT	TCGGGA	TCCCGA
47	CAAGCAGAAGACGGCATAACGAGATCTTCGAATTTATACCATTTTAATTCAGCTTTGT	CTTCGA	TCGAAG
48	CAAGCAGAAGACGGCATAACGAGATTGCCGAATTTATACCATTTTAATTCAGCTTTGT	TGCCGA	TCGGCA
49	CAAGCAGAAGACGGCATAACGAGATTAGCGCATTTATACCATTTTAATTCAGCTTTGT	TAGCGC	GCGCTA
50	CAAGCAGAAGACGGCATAACGAGATGTGTTTATTTATACCATTTTAATTCAGCTTTGT	GTGTTT	AAACAC
51	CAAGCAGAAGACGGCATAACGAGATCCTTCAATTTATACCATTTTAATTCAGCTTTGT	CCTTCA	TGAAGG
52	CAAGCAGAAGACGGCATAACGAGATTATGTTATTTATACCATTTTAATTCAGCTTTGT	TATGTT	AACATA
53	CAAGCAGAAGACGGCATAACGAGATGACGCGATTTATACCATTTTAATTCAGCTTTGT	GACGCG	CGCGTC
54	CAAGCAGAAGACGGCATAACGAGATTGTATCATTTATACCATTTTAATTCAGCTTTGT	TGTATC	GATACA
55	CAAGCAGAAGACGGCATAACGAGATCACACCATTTATACCATTTTAATTCAGCTTTGT	CACACC	GGTGTG
56	CAAGCAGAAGACGGCATAACGAGATTTCTTAATTTATACCATTTTAATTCAGCTTTGT	TTCTTA	TAAGAA
57	CAAGCAGAAGACGGCATAACGAGATCTCGCTATTTATACCATTTTAATTCAGCTTTGT	CTCGCT	AGCGAG
58	CAAGCAGAAGACGGCATAACGAGATTAACCGATTTATACCATTTTAATTCAGCTTTGT	TAACCG	CGGTTA
59	CAAGCAGAAGACGGCATAACGAGATAAAGCTATTTATACCATTTTAATTCAGCTTTGT	AAAGCT	AGCTTT
60	CAAGCAGAAGACGGCATAACGAGATAGACCAATTTATACCATTTTAATTCAGCTTTGT	AGACCA	TGGTCT
61	CAAGCAGAAGACGGCATAACGAGATGGGATAATTTATACCATTTTAATTCAGCTTTGT	GGGATA	TATCCC
62	CAAGCAGAAGACGGCATAACGAGATACGACAATTTATACCATTTTAATTCAGCTTTGT	ACGACA	TGTCGT
63	CAAGCAGAAGACGGCATAACGAGATGTGGGGATTTATACCATTTTAATTCAGCTTTGT	GTGGGG	CCCCAC
64	CAAGCAGAAGACGGCATAACGAGATTCGTATATTTATACCATTTTAATTCAGCTTTGT	TCGTAT	ATACGA

65	CAAGCAGAAGACGGCATAACGAGATCAAGGGATTTATACCATTTTAATTCAGCTTTGT	CAAGGG	CCCTTG
66	CAAGCAGAAGACGGCATAACGAGATGCCGGTATTTATACCATTTTAATTCAGCTTTGT	GCCGGT	ACCGGC
67	CAAGCAGAAGACGGCATAACGAGATCAGTAAATTTATACCATTTTAATTCAGCTTTGT	CAGTAA	TTACTG
68	CAAGCAGAAGACGGCATAACGAGATAGTTCCATTTATACCATTTTAATTCAGCTTTGT	AGTTCC	GGAACT
69	CAAGCAGAAGACGGCATAACGAGATAATAACATTTATACCATTTTAATTCAGCTTTGT	AATAAC	GTTATT
70	CAAGCAGAAGACGGCATAACGAGATACTTTTATTTATACCATTTTAATTCAGCTTTGT	ACTTTT	AAAAGT
71	CAAGCAGAAGACGGCATAACGAGATTCCTTATTTATACCATTTTAATTCAGCTTTGT	TCCCTT	AAGGGA
72	CAAGCAGAAGACGGCATAACGAGATATACTTATTTATACCATTTTAATTCAGCTTTGT	ATACTT	AAGTAT
73	CAAGCAGAAGACGGCATAACGAGATAGATGTATTTATACCATTTTAATTCAGCTTTGT	AGATGT	ACATCT
74	CAAGCAGAAGACGGCATAACGAGATAATCGTATTTATACCATTTTAATTCAGCTTTGT	AATCGT	ACGATT
75	CAAGCAGAAGACGGCATAACGAGATCGGCGTATTTATACCATTTTAATTCAGCTTTGT	CGGCGT	ACGCCG
76	CAAGCAGAAGACGGCATAACGAGATGAGAGTATTTATACCATTTTAATTCAGCTTTGT	GAGAGT	ACTCTC
77	CAAGCAGAAGACGGCATAACGAGATGATTCTATTTATACCATTTTAATTCAGCTTTGT	GATTCT	AGAATC
78	CAAGCAGAAGACGGCATAACGAGATCCCAATATTTATACCATTTTAATTCAGCTTTGT	CCCAAT	ATTGGG
79	CAAGCAGAAGACGGCATAACGAGATACGCGGATTTATACCATTTTAATTCAGCTTTGT	ACGCGG	CCGCGT
80	CAAGCAGAAGACGGCATAACGAGATAGGGCGATTTATACCATTTTAATTCAGCTTTGT	AGGGCG	CGCCCT
81	CAAGCAGAAGACGGCATAACGAGATCTGCAGATTTATACCATTTTAATTCAGCTTTGT	CTGCAG	CTGCAG
82	CAAGCAGAAGACGGCATAACGAGATAACTTCATTTATACCATTTTAATTCAGCTTTGT	AACTTC	GAAGTT
83	CAAGCAGAAGACGGCATAACGAGATGGGTGCATTTATACCATTTTAATTCAGCTTTGT	GGGTGC	GCACCC
84	CAAGCAGAAGACGGCATAACGAGATTCCTGCATTTATACCATTTTAATTCAGCTTTGT	TCCTGC	GCAGGA
85	CAAGCAGAAGACGGCATAACGAGATCGCGGCATTTATACCATTTTAATTCAGCTTTGT	CGCGGC	GCCGCG
86	CAAGCAGAAGACGGCATAACGAGATACCGCCATTTATACCATTTTAATTCAGCTTTGT	ACCGCC	GGCGGT
87	CAAGCAGAAGACGGCATAACGAGATTAATACATTTATACCATTTTAATTCAGCTTTGT	TAATAC	GTATTA
88	CAAGCAGAAGACGGCATAACGAGATCACGTAATTTATACCATTTTAATTCAGCTTTGT	CACGTA	TACGTG
89	CAAGCAGAAGACGGCATAACGAGATATGTGAATTTATACCATTTTAATTCAGCTTTGT	ATGTGA	TCACAT

**Name**

**Sequences**

NGS-F3 AATGATACGGCGACCACCGAGATCTACACTCTTTCCCTACACGACGCTCTTCCGATCTNNNNCATGGACGAGCTGTACAAGT  
 Forward amplification primer

**Supplementary Table 5. Primer sequences.**

<b>Gene</b>	<b>Seq</b>
LCK-F	CACGCTGCTCATCCGAAATG
LCK-R	ACCAGGTTGTCTTGCAGTGG
PTCRA-F	TGGATGCCTTCACCTATGGC
PTCRA-R	AAGCCTCTCCTGACAGATGC
ZAP70-F	GAACTTTGTGCACCGTGACC
ZAP70-R	CTGAGCGGGCAGTGTAGTAG
FYN-F	TACCCAGGCATGAACAACCG
FYN-R	GTTGGTACTGGGGCTCTGTC
GILZ-F	CATGGAGGTGGCGGTCTA
GILZ-R	TTACACCGCAGAACCACCAG

Supplementary Table 6. Patient and cell line characteristics.

UPN	Gender	Age (years)	Time-point	White cell count (10E-9/L)	Cytogenetics	Subgroup	Molecular
L809	Male	16	diagnosis	319	46,XY,del(6)(q13q23). Extra RUNX1 signal [11%]	TAL1	nk
L903	Female	4	diagnosis	nk	46,XX. STIL-TAL1	TAL1	nk
L907	Male	12	diagnosis	nk	46,XY	TAL2	nk
L963	Male	4	diagnosis	104	46,XY,r(5)(p14q23),del(7)(q22)	nk	nk
L970	Male	11	diagnosis	316	t(5;14)(q35;q32) BCL11B-TLX3	TLX3	nk
LK080	Male	1	relapse	19	46,XY	nk	nk
LK203	Female	4	diagnosis	760	46,XX	TCRA-LMO2?	Deletion CDKN2A, PTEN
LK287	Male	15	diagnosis	272	46,XY,del(6)(q14~16q23). STIL-TAL1. FIP1L1-PDGFR.A.	TAL1	nk
LK290	Male	15	diagnosis	75	46,XY. t(11;19)(q23;p13.3) KMT2A-MLLT1	KMT2A	nk

nk = not known

Cell line	Gender	Age (years)	Disease	ATCC / DSMZ	Cytogenetics	TCR status	Mutation	Deletion
SUPT1	Male	8	T-LBL	CRL 1942	t(7;9)(q34;q34.3)	pTCR+		CDKN2B
			Relapse		TRB-NOTCH1/TAN1	TCRαβ-		CDKN2A
					Inv(14)(q11q32)			
CUTLL1	Male	14	T-NHL		TRAD-IGH			
			Relapse		t(7;9)(q34;q34)	TCRαβ+	TP53	
					TRB-NOTCH			
HPB-ALL	Male	14	T-ALL	ACC 483	t(5;14)(q35;q32.2)	TCRαβ+		IFNB
			Diagnosis		HOX11L2/TLX3-BCL11B			CDKN2B
					pseudodiploid with 8% polyploidy			CDKN2A
HSB-2	Male	11	T-ALL	ACC 435	t(1;7)(p34;q34)	TCRαβ-	LCK <sup>V28L</sup>	
					LCK-TRB		LCK <sup>A353V</sup>	
					submicroscopic del(1)(p32)		LCK <sup>P447L</sup>	
					STIL-TAL1(SIL-SCL)		LCK p.232_233insQKP	
					pseudodiploid with 4% polyploidy			
MOLT4	Male	19	T-ALL	CRL 1582	hypertetraploid	TCRαβ-	NRAS	CDKN2A
			Relapse	ACC 362		pTCR+	TP53	
							PTEN	
Jurkat	Male	14	T-ALL	TIB 152	pseudodiploid	TCRαβ+	TP53 p.T125T	IFNA
			Relapse				PTEN p.R234fs, p.L247fs	CDKN2B CDKN2A
							LCK p.L251fs	
MOLT16	Female	5	T-ALL	ACC 29	t(8;14)(q24;q11)	TCRαβ+	TP53	CDKN2B CDKN2A
			Relapse		MYC-TRAD <sub>1</sub>		PTEN	
					submicroscopic del(1)(p32) SIL-TAL1/SCL fusion			
				near-diploid				
KOPT-K1	Male	6	T-NHL		t(11;14)(p13;q11) LMO2/TTG2-TRD	TCRαβ-		CDKN2A
DU.528	Male	16	T-ALL	40625	t(1;14)(p32;q11)	TCRαβ-		
			Diagnosis		TAL1/SCL-TRD			
ALLSIL	Male	17	T-ALL	ACC 511	t(10;14)(q24;q11) TLX1/HOX11-TRAD	TCRαβ-		IFNA
			Relapse		NUP214-ABL1			IFNB
					hypertetraploid			CDKN2B
								CDKN2A
CCRF-CEM	Female	3	T-ALL	CCL 119	submicroscopic del(1)(p32)	TCRαβ+	TP53	IFNA
			Relapse	ACC 240	SIL-TAL1/SCL		KRAS	IFNB
					t(5;14)(q35.1;q32.2)			CDKN2A
					NKX2-5-BCL11B			
				near-tetraploid				